

# **ELECTROCOAGULATION FOR PHOSPHORUS RECOVERY FROM ANAEROBIC EFFLUENT**

by

**Gyana Prakash Bhoi**

Bachelor of Technology in Civil Engineering

Biju Patnaik University of Technology, Rourkela, India, 2015-2019

A Thesis Submitted in Partial Fulfillment of  
the Requirements for the Degree of

**Master of Science in Engineering**

in the Graduate Academic Unit of Civil Engineering

Supervisor: Kripa S. Singh, Ph.D., P.Eng., Department of Civil Engineering

Examining Board: Bruce Wilson, Ph.D., P.Eng., Department of Civil Engineering

Othman Nasir, Ph.D., P.Eng., Department of Civil Engineering

Gobinda Saha, Ph.D., P.Eng., Department of Mechanical Engineering

This thesis is accepted by the Dean of Graduate Studies

THE UNIVERSITY OF NEW BRUNSWICK

August 2022

© Gyana Prakash Bhoi, 2022

## ABSTRACT

A batch monopolar electrocoagulation system was developed to compare the performance of iron and magnesium electrocoagulation systems for phosphorus recovery from anaerobic bioreactor effluent and to understand the effects of parameters such as initial pH, retention time, current density, inter-electrode distance, as well as their interactions. For iron electrocoagulation system, removal of 98.05 % total phosphorus (TP) was observed at optimal operating conditions (pH=6.75, retention time=11.06 min, current density=300 A/m<sup>2</sup>, inter-electrode distance=1.5 cm). A kinetic study for TP removal revealed that at optimal conditions, phosphorus removal followed first-order kinetics (rate constant(K)=0.185 m/min). Phosphorus was recovered from the post-precipitated iron electrocoagulation sludge through combustion followed by acid leaching. Acid leaching tests using sulphuric acid resulted in around 91% of phosphorus recovery at a liquid-to-solid ratio of 100 mL/g with sulphuric acid. However, for magnesium electrocoagulation system, TP recovery of 97.3% was observed at optimal conditions (pH=8.4, retention time=35 min, current density=300 A/m<sup>2</sup>, and inter-electrode distance=0.5 cm). The energy consumption for iron and magnesium electrocoagulation systems under optimal conditions was found to be 1.28 kWh/m<sup>3</sup> and 2.35 kWh/m<sup>3</sup>, respectively. A kinetic study for TP removal revealed that at optimum operating conditions, TP removal followed second-order kinetics (rate constant(K)=0.0117 mg/(m<sup>2</sup>·min)). X-ray Diffraction analysis of the iron electrocoagulation sludge was found to be amorphous whereas for magnesium precipitate revealed the presence of struvite as the only crystalline compound.

## DEDICATION

I dedicate this thesis to my parents Susheel Bhoi and Pratima Bhoi, as well as my cousin Ashirbad Pradhan for their constant support, help and belief throughout the length of the project.

## ACKNOWLEDGEMENTS

I would like to thank the following funding agencies: the Natural Science and Engineering Research Council (NSERC), the New Brunswick Innovation Foundation (NBIF), the University of New Brunswick (UNB).

I consider myself extremely fortunate for the opportunity to learn and work under the supervision of Dr. Kripa Singh over the duration of the program. His valuable guidance, support, and teachings throughout the length of the project helped me achieve this objective.

I would also like to personally thank:

- Dr. Dennis Connor for his technical assistance and knowledge throughout the project.
- Mohit Bhargav for helping me with chemical analyses in the laboratory at different times during the research.
- Greg Greer for the fabrication of the electrodes.
- Ven Reddy for the XRD analysis and Steven Cogswell for the SEM analysis.
- Ms. Runu Singh for her support throughout the length of the program.
- Other friends and family members for their constant support.

# TABLE OF CONTENTS

<b>ABSTRACT .....</b>	<b>ii</b>
<b>DEDICATION .....</b>	<b>iii</b>
<b>ACKNOWLEDGEMENTS .....</b>	<b>iv</b>
<b>TABLE OF CONTENTS.....</b>	<b>v</b>
<b>LIST OF TABLES .....</b>	<b>viii</b>
<b>LIST OF FIGURES .....</b>	<b>ix</b>
<b>LIST OF ABBREVIATIONS .....</b>	<b>x</b>
<b>1. Introduction.....</b>	<b>1</b>
1.1 Background and Problem Statements .....	1
1.2 Objectives.....	4
1.3 Scope of the Research.....	4
1.4 Organization of the Thesis.....	6
<b>2. Literature Review.....</b>	<b>8</b>
2.1 Occurrence of Phosphorus in the Environment .....	8
2.2 Wastewater and Struvite .....	9
2.3 Methods for Phosphorus Recovery.....	11
2.3.1 Electrochemical Method.....	11
2.3.2 Chemical Precipitation .....	13
2.3.3 Biological Phosphorus Removal.....	14
2.3.4 Adsorption .....	16
2.4 Electrocoagulation Principles.....	17
2.4.1 Advantages of Electrocoagulation .....	19
2.4.2 Disadvantages of Electrocoagulation .....	20
2.4.3 Electrodes Arrangement.....	21
2.5 Factors affecting Electrocoagulation.....	23
2.5.1 Initial pH.....	23
2.5.2 Retention Time .....	24
2.5.3 Current Density.....	25
2.5.4 Inter-electrode Distance .....	26
2.6 Response Surface Methodology.....	26

2.6.1 Central Composite Design .....	28
<b>3. Materials and Methods.....</b>	<b>30</b>
3.1 Anaerobic Bioreactor Effluent and Characteristics .....	30
3.2 Experimental Setup and Operation.....	30
3.3 Development of Central Composite Design.....	33
3.4 Analytical Methods.....	34
3.4.1 Total Phosphorus (TP).....	34
3.4.2 Chemical Oxygen Demand (COD) .....	34
3.4.4 pH.....	34
3.4.5 Ammonia-Nitrogen (NH <sub>3</sub> -N).....	35
3.4.6 XRD Analysis.....	35
3.4.7 SEM Analysis .....	35
3.4.8 Data Collection.....	35
3.4.9 Data Analysis.....	36
3.4.10 Quality Control.....	36
3.5 Optimization .....	37
<b>4. Results and Discussion .....</b>	<b>38</b>
4.1 Iron Electrocoagulation System .....	38
4.1.1 Statistical Analysis.....	39
4.1.2 Effect of Independent Process Variables.....	42
4.1.3 Variable Interaction and Response.....	45
4.1.4 Effect on COD Removal.....	49
4.2 Magnesium Electrocoagulation System.....	52
4.2.1 Statistical Analysis.....	53
4.2.2 Effect of Independent Process Variables.....	57
4.2.3 Variable Interaction and Response.....	60
4.2.4 Effect on COD Removal.....	64
4.2.5 Effect on Ammonia-Nitrogen Removal.....	66
4.3 Optimization .....	69
4.3.1 Optimization for Fe-Electrocoagulation System.....	69
4.3.2 Optimization for Mg-Electrocoagulation System .....	71
4.4 Kinetics of TP Removal .....	73
4.4.1 Iron Electrocoagulation System.....	73

4.4.2 Magnesium Electrocoagulation System .....	75
4.5 Acid Leaching.....	76
<b>5. Conclusions, Recommendations and Applications to Practice .....</b>	<b>78</b>
5.1 Conclusions.....	78
5.2 Recommendations for Future Work .....	79
5.3 Applications to Practice .....	80
<b>REFERENCES .....</b>	<b>81</b>
<b>Appendix A: TP Data .....</b>	<b>92</b>
<b>Appendix B: EDS Analysis.....</b>	<b>94</b>
<b>Curriculum Vitae</b>	

## LIST OF TABLES

Table 1: Efficacy of EC on various types of wastewater .....	12
Table 2: Characteristics of anaerobic effluent .....	30
Table 3: Independent variables and levels: Iron EC runs .....	33
Table 4: Independent variables and levels: Magnesium EC runs .....	34
Table 5: Data collection frequency .....	35
Table 6: Design matrix: Iron EC runs .....	38
Table 7: Model summary: Iron EC runs.....	40
Table 8: ANOVA results: Iron EC runs .....	40
Table 9: COD removal data: Iron EC runs.....	51
Table 10: Design matrix: Magnesium EC runs .....	52
Table 11: Model summary: Magnesium EC runs .....	54
Table 12: ANOVA results: Magnesium EC runs.....	54
Table 13: COD removal data: Magnesium EC runs .....	65
Table 14: NH <sub>3</sub> -N removal data: Magnesium EC runs .....	68
Table 15: Verification of experimental results: Iron EC runs .....	69
Table 16: Verification of experimental results: Magnesium EC runs.....	71
Table 17: Significant factors for EC systems .....	78
Table 18: TP data: Iron EC runs .....	92
Table 19: TP data: Magnesium EC runs.....	93

## LIST OF FIGURES

Figure 1: Mechanism of electrocoagulation .....	17
Figure 2: Electrodes arrangement.....	22
Figure 3: Central composite design .....	29
Figure 4: Schematic of the EC batch reactor setup.....	32
Figure 5: Photograph of the EC batch reactor setup .....	32
Figure 6: Predicted vs Observed TP removal efficiency.....	41
Figure 7: Factorial plots for TP removal: Iron EC runs .....	45
Figure 8: Response surface plots for TP removal: Iron EC runs .....	47
Figure 9: Contour plots for TP removal: Iron EC runs .....	48
Figure 10: Factorial plots for COD removal: Iron EC runs .....	50
Figure 11: Normal probability plot of the residuals.....	55
Figure 12: Predicted vs Observed TP recovery efficiency.....	56
Figure 13: Factorial plots for TP recovery: Magnesium EC runs .....	59
Figure 14: Response surface plots for TP recovery: Magnesium EC runs.....	62
Figure 15: Contour plots for TP recovery: Magnesium EC runs.....	63
Figure 16: Factorial plots for COD removal: Magnesium EC runs.....	64
Figure 17: Factorial plots for NH <sub>3</sub> -N removal: Magnesium EC runs.....	67
Figure 18: XRD spectra of the iron EC sludge.....	70
Figure 19: SEM image of the iron EC sludge .....	70
Figure 20: XRD spectra of the magnesium EC sludge .....	72
Figure 21: Electron micrograph of struvite crystals .....	73
Figure 22: Ln(C <sub>t</sub> ) vs time.....	74
Figure 23: 1/TP vs time .....	75
Figure 24: Effect of L/S ratio on phosphorus yield.....	77
Figure 25: EDS analysis of the iron EC sludge .....	94
Figure 26: EDS analysis of the magnesium EC sludge .....	95

## LIST OF ABBREVIATIONS

CCD: Central Composite Design

CD: Current Density

COD: Chemical Oxygen Demand

EC – Electrocoagulation

EDS: Energy-Dispersive X-ray Spectroscopy

fCOD: Filtered Chemical Oxygen Demand

Fe: Iron

I: Current

E: Voltage

V: Reactor Volume

ICP-OES: Inductively Coupled Plasma - Optical Emission Spectrometry

IED: Inter-electrode Distance

K: Rate Constant

L/S: Liquid-to-Solid

Mg: Magnesium

M<sup>2+</sup>: Metal ion

NH<sub>3</sub>-N: Ammonia-Nitrogen

OVAT: One Variable at a Time

RSM: Response Surface Methodology

RT: Retention Time

SEM: Scanning Electron Microscopy

TP: Total Phosphorus

WASSTRIP: Waste Activated Sludge Stripping

XRD: X-ray Diffraction

# 1. Introduction

## 1.1 Background and Problem Statements

Phosphorus (P), an essential element for all living organisms, is obtained for agricultural and industrial purposes, primarily from phosphate rock (phosphorite). As phosphate is a limited and non-renewable resource, a rapid increase in phosphate consumption can put enormous strain on the global phosphate rock reserves. It is estimated that the global phosphate reserves will be depleted in ten decades if current phosphate mining rates continue and no intervention measures are adopted (Gilbert, 2009). The agricultural sector accounts for 85% of phosphorus consumption (Johnston et al., 2014). Furthermore, global phosphorus consumption has gradually increased from 43.7 million tonnes in 2015 to 48.2 million tonnes in 2019 (Hermann et al., 2018). To deal with the scarcity of phosphorus, it is crucial to identify alternate phosphorus sources. Phosphorus levels in anaerobic digestate (Huang et al., 2017), municipal wastewater (Yuan et al., 2012), and agro-industry wastes (Moerman et al., 2009) are typically very high. The recovery of phosphate from these waste streams is an attractive option for achieving long-term phosphorus supplies. These sources have the potential to account for 15-20% of global P demand (Yuan et al., 2012).

Excess phosphorus in the water bodies causes eutrophication. This also leads to depletion of dissolved oxygen and generates toxins in the water, resulting in the death of aquatic organisms and causing damage to wildlife (Conley et al., 2009; Li et al., 2016).

The presence of phosphorus in the waste stream encourages fouling of water pipes, resulting in costly maintenance (Attour et al., 2014). Moreover, the presence of phosphorus in wastewater causes uncontrolled struvite formation in pipes, which causes clogging and raises wastewater plant maintenance costs (Le Corre et al., 2009). Therefore, recovery or removal of phosphate from wastewater discharges is important to maintain a balance of phosphorus in the aquatic environment.

Among the available methods, chemical and biological phosphorus recovery methods are widely used industrially and can achieve a low phosphorus concentration in the treated effluent (Li et al., 2019; Wang et al., 2018; Yin et al., 2015). However, these procedures are energy-intensive and need large amounts of chemicals used as a coagulant. Furthermore, chemical coagulation is associated with high sludge production (Sengupta et al., 2015), whereas biological phosphorus removal requires complex configuration and operating regimes (Bowker & Stensel, 1990). These shortcomings sparked the interest of researchers in exploring other alternatives for sustainable phosphorus recovery from anaerobic effluent.

One proposed solution to deal with this problem is electrocoagulation. This process has the potential to significantly reduce the addition of external coagulants while achieving high removal efficiency. Moreover, commercially available technologies such as Ostara and AirPrex use the chemical precipitation method for phosphorus recovery as struvite (OSTARA, 2017; P-Rex, 2015). Electrocoagulation has yet to be applied in industry for phosphorus recovery. Several studies on phosphorus removal using an electrocoagulation system have been published. In the majority of the studies, synthetic

wastewater was used, which avoids the interaction of other constituent ions such as COD with the process of phosphorus removal (Bakshi et al., 2020; Gharibi et al., 2010; Zeng et al., 2021). Studies are deficient in exploring the interaction of parameters such as pH and current density (Huang et al., 2017; Tran et al., 2012). These parameters affect the mass of metal ion generation from the anode. Moreover, studies on phosphorus recovery using magnesium electrocoagulation system are scarce. In the present study comparative evaluation of the removal and recovery of phosphorus using iron and magnesium electrodes, kinetics of phosphorus removal, and optimization of process parameters are presented. The magnesium EC process could serve as a better alternative for struvite precipitation compared to the existing process i.e., chemical precipitation.

Recently, the electrochemical method of phosphorus removal and recovery has gained considerable research interest due to an increased requirement for wastewater discharge with respect to phosphorus as well as stringent guidelines (TP < 1mg/L) for wastewater disposal, especially from the on-site septic systems in rural areas of Canada (Devlin et al., 2019; Gaurina-Medjimurec, 2015; Environment Canada, 2006). Furthermore, its ease of use and high efficiency are other contributing factors to its popularity (Lacasa et al., 2011). Electrocoagulation has already been employed to treat compost leachate (Dastyar et al., 2015), swine wastewater (Mores et al., 2016), and domestic wastewater (Omwene & Kobya, 2018) as a polishing step for many biological treatment processes.

## 1.2 Objectives

The main goal of this study is to develop a batch monopolar electrocoagulation system to recover phosphorus from anaerobic bioreactor effluent from a potato processing wastewater treatment plant.

The objectives of the study are as follows:

1. To compare the phosphorus recovery performance of iron (Fe) and magnesium (Mg) electrodes.
2. To evaluate the potential of the electrocoagulation process to remove phosphorus from anaerobic bioreactor's effluent under various operating conditions (initial pH, current density, retention time and inter-electrode distance).
3. To conduct a statistical optimization of independent process variables to maximize the total phosphorus (TP) removal and to model response and prediction using response surface methodology (RSM).
4. To recover phosphorus from the precipitates formed during the electrocoagulation process using combustion followed by an acid leaching process.
5. To evaluate the impact of Electrocoagulation on COD removal for iron and magnesium electrodes, as well as the impact of a magnesium electrocoagulation system on ammonia removal.

## 1.3 Scope of the Research

The following tasks were undertaken to conduct the study:

Task 1 was to design a bench scale batch EC reactor using two different types of electrode

materials (iron and magnesium) to investigate the effects of physio-chemical parameters such as initial pH, retention time, current density and inter-electrode distance on phosphorus removal and recovery.

Task 2 was to define the range of independent process variables based on the literature and preliminary studies. More details regarding the ranges of the independent variables for both iron and magnesium EC systems are presented in Chapter 3. This study was designed using a central composite design with five levels. Experimental run parameters were obtained using Minitab 20 software.

Task 3 was to fit a quadratic model to the experimental data using multiple regression analysis. This model functions as a predictive model, predicting total phosphorus removal for a given set of operating conditions. The response surface and contour plots were used to better understand the effect of independent process variables and their interactions on total phosphorus removal efficiency.

Task 4 was to investigate the effect of electrocoagulation on COD removal efficiency in iron and magnesium electrocoagulation systems, as well as ammonia ( $\text{NH}_3\text{-N}$ ) removal in magnesium electrocoagulation system.

Task 5 involved optimization of the independent process variables using response surface methodology to maximize total phosphorus removal/recovery efficiency.

Task 6 entailed conducting kinetic studies at optimal conditions for both iron and magnesium batch EC systems to understand the rate of phosphorus removal.

Task 7 was to apply combustion followed by acid leaching on iron EC sludge obtained from optimal runs for phosphorus extraction. Acid leaching tests were carried out to determine the effect of various liquid-to-solid (L/S) ratios (50 mL/g, 100 mL/g, 150 mL/g, and 200 mL/g) on phosphorus yield.

## 1.4 Organization of the Thesis

The thesis is organized into five chapters as follows:

The first chapter discusses the background and significance of resource recovery, as well as the problem statement, research objectives, and scope of the research, followed by the organization of the thesis.

The second chapter presents a review of the literature for the research project, which focuses on the occurrence of phosphorus in the environment, electrocoagulation principles, benefits, drawbacks, and a detailed description of the factors influencing the process. This chapter also includes a description of the response surface methodology as well as the available methods for phosphorus recovery.

The third chapter covers information related to variables, experimental setup and procedure, development of central composite design, associated instruments along with analytical methods.

The fourth chapter discusses the results obtained for the iron and magnesium electrocoagulation system, as well as the optimization for independent process variables and kinetics of total phosphorus removal. This chapter also includes acid leaching for the precipitates obtained from the iron electrocoagulation system. The research findings for

the effect of initial pH, retention time, current density and inter-electrode distance on TP removal was presented at the 2021 Virtual Atlantic and Eastern Canadian Symposium on Water Quality. These research findings were also submitted to the Water Quality Research Journal (IWA Publishing) for peer review. A second referred journal publication on the findings of the electrocoagulation using magnesium electrodes, as well as a comparison of its performance with the iron electrodes is in preparation.

The fifth chapter contains the conclusion of the overall research findings as well as suggestions for future research. Additionally, the application of the research project's results is discussed.

## 2. Literature Review

### 2.1 Occurrence of Phosphorus in the Environment

Phosphorus occurs in the wastewater in two forms: organic P (polyphosphate) and inorganic form (ortho phosphate), which can be dissolved or suspended (Schnug & De Kok, 2016). Accumulation of phosphorus in water bodies can take place from both urban and agricultural sources. These sources can be classified as point sources and non-point sources. The concentration of phosphate in domestic wastewater typically ranges from 3 mg/L to 11mg/L (Metcalf & Eddy, 2014). In biological wastewater treatment, the activated sludge produced during the treatment has high nutrient content. Anaerobic digestion of the waste activated sludge causes the release of phosphorus as phosphate and nitrogen as ammonia nitrogen into the effluent (Münch & Barr, 2001). Phosphorus levels in anaerobic digestate/anaerobic bioreactor effluent (Huang et al., 2017), municipal wastewater (Yuan et al., 2012), and agro-industry wastes (Moerman et al., 2009) are typically high.

The presence of substantial quantities of phosphorus in the water bodies causes eutrophication, which interferes with the reproduction of algae and microorganisms (Conley et al., 2009; Li et al., 2016). Eutrophication is defined as uncontrolled plant and algal growth caused by an abundance of limiting growth factor such as nutrients (nitrogen and phosphorus). An adequate concentration of phosphorus promotes vegetation and the growth of soil microbes whereas its abundance can lead to water quality issues. This depletes dissolved oxygen and generates toxins in the water, resulting

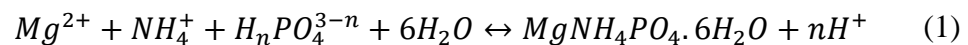
in the death of aquatic organisms and causing damage to wildlife (Li et al., 2016; Conley et al., 2009) and can become a public health concern. The presence of phosphorus in the waste stream encourages fouling of water pipes, resulting in costly maintenance (Attour et al., 2014). As a result, environmental regulations have recently become more stringent in order to limit phosphorus concentrations in the aquatic environment. According to wastewater discharge guidelines issued by Environment Canada, the wastewater treatment plant effluent should be less than the monthly average limit of 1 mg/L total phosphorus (Environment Canada, 2006).

## 2.2 Wastewater and Struvite

Wastewater treatment plants are required to remove phosphorus in order to achieve desired discharge limits, prior to discharging wastewater into receiving water bodies. Conventional method of phosphorus removal involves the addition of coagulants such as ferric sulfate ( $\text{Fe}_2(\text{SO}_4)_3$ ), ferric chloride ( $\text{FeCl}_3$ ), and aluminium sulfide ( $\text{Al}_2\text{S}_3$ ). However, in the precipitate formed as a result of this process, phosphorus is bound to metal ions such as Fe and Al making it unavailable for plants (Kyle & McClintock, 1995). This precipitate needs to be processed further for phosphorus extraction for agricultural and industrial applications. Whereas phosphorus recovery as struvite can be beneficial in terms of removing phosphorus from wastewater and direct application of precipitate (i.e., struvite) as a fertilizer. Struvite is a popular slow-release fertilizer due to the availability of nutrients such as nitrogen and phosphorus. It has already been used in agriculture and has been discovered that it improves nutrient uptake by plants while having no negative effects ( Zhang et al., 2010). Slow-release fertilizers are water

insoluble at neutral pH, resulting in little to no nutrient production during agricultural runoff. When compared to conventional fertilizers, it has a very low contribution to eutrophication (Ohlinger et al., 1999).

Struvite is a poorly soluble crystalline substance composed of equimolar concentrations of magnesium, ammonium, and phosphate. It was named after the geologist Von Struve (1772-1851), who discovered it. It has a molecular weight of 245.41 g/mol. It is a fine white powder with high solubility in acidic pH, but it is highly insoluble at pH above 7. Due to the fact that struvite precipitation is affected by initial pH, alkalinity and trace element concentrations, this molar ratio cannot be used to calculate the magnesium dosage required for this process (Metcalf & Eddy 2003). The general equation for struvite formation is as shown in equation (1) (Le Corre et al., 2009). The value for n varies from 0 to 2.



Struvite crystallization using a magnesium electrocoagulation system avoids the necessity of the addition of magnesium as a chemical source. Instead of adding chemicals, this process involves the addition of  $Mg^{2+}$  ions from the anode by anodic dissolution, under the application of electric current. Struvite precipitation is primarily dependent on the initial pH and the concentration of  $Mg^{2+}$  ions. Initial pH affects the solubility of struvite formed during the reaction.

Controlled chemical struvite precipitation was initially investigated to avoid scaling issues in the wastewater treatment process (Stratful et al., 1999). This process has been in use at Shimane Prefecture Works in Japan since 1998 which uses digester

supernatant of initial phosphorus concentration of around 100 mg/L (Ueno & Fujii, 2001). Ostara technology developed at the University of British Columbia, Canada recovers phosphorus from nutrient-rich wastewater for struvite precipitation and sells the struvite as Crystal Green, a premium fertilizer (OSTARA, 2017). This method is already being used in 14 different facilities around the world. This method is based on the principle of WASSTRIP (Waste Activated Sludge Stripping to Recover Internal Phosphate) and Pearl. The WASSTRIP process is used to release nutrients such as phosphate and ammonia from the sludge whereas the Pearl process involves addition of NaOH to raise the pH and magnesium salts to facilitate struvite production (OSTARA, 2017). Another method AirPrex was developed by Berliner Wasserbetriebe which involves struvite precipitation from the sludge stream. This process involves addition of  $MgCl_2$  as the magnesium source.

## 2.3 Methods for Phosphorus Recovery

### 2.3.1 Electrochemical Method

Electrochemical methods of nutrient recovery such as electrocoagulation, electrooxidation and electrodialysis are the emerging technologies for the treatment of wastewater as well as for nutrient recovery. Electrocoagulation can be applied for the removal of a range of pollutants and wastewater treatment. Several researchers have investigated the feasibility of treating industrial and municipal wastewater with electrocoagulation process. The efficiency of the electrocoagulation system for phosphorus removal was compared to previous studies treating various types of

wastewaters with different electrode materials. Operating parameters for the studies are shown in Table 1.

**Table 1: Efficacy of EC on various types of wastewater**

S. No	Type of Wastewater	Optimum Conditions				Electrode Material	TP Removal Efficiency (%)	References
		pH	RT (mins)	I/E/ CD	IED (cm)			
1	Sludge Anaerobic supernatant	3	80	37.5 A/m <sup>2</sup>	2	Fe	99	Huang et al. (2017)
2	Municipal Wastewater	7	20	382 A/m <sup>2</sup>	1	Mild steel	97	Tran et al. (2012)
3	Palm Oil Mill Effluent	6.4	7.69	77.8 A/m <sup>2</sup>	-	Fe	73	Damaraju et al. (2019)
4	Synthetic	7	14	11.5 V	3	Scrap Al	90	Bakshi et al. (2020)
5	Dairy Manure	7.4	100	0.6 A	4	Low Carbon Steel	96.7	Zhang et al. (2016)
6	Synthetic	5.5	40	40 V	1.5	Fe	>99	Gharibi et al. (2010)
7	Synthetic	7.4	34	21 A/m <sup>2</sup>	1.8	Fe	90.24	Zeng et al. (2021)
8	Anaerobic bioreactor effluent	6.75	11.06	300 A/m <sup>2</sup>	1.5	Fe	98.05	Present Study
		8.4	35	300 A/m <sup>2</sup>	0.5	Mg	97.30	
9	Synthetic	7	240	55 A/m <sup>2</sup>	3	Mg	98%	Kim et al. (2018)
10	Synthetic	7.5	120	45 A/m <sup>2</sup>	-	Mg	98	Kruk et al. (2014)
11	Industrial wastewater	7.1	90	440 A/m <sup>2</sup>	1	Mg	98.5%	Carmona-Carmona et al. (2021)

\*I=current, E= voltage

Electrocoagulation process of phosphorus recovery has several benefits over the traditional method of phosphorus removal methods. Coagulation and flotation occur concurrently during the process, giving it a clear advantage over chemical precipitation (Mollah et al., 2001). From table 1, it can be seen that this method is capable of removing more than 90% phosphorus at optimum conditions and can help to achieve low phosphorus concentration to meet discharge guidelines. Moreover, this method involves a simple reactor configuration with high treatment efficiency (Lacasa et al., 2011). It can be conducted in a small treatment plant resulting in low cost with complete automation as coagulant dosing is controlled electrically. This process is advantageous for small, localized water treatment and can be operated using solar energy (Vasudevan et al., 2009). The electrocoagulation process is described in detail in section 2.4.

### 2.3.2 Chemical Precipitation

Chemical P removal involves the addition of metal ions in the form of salt, which reacts with the inorganic phosphates dissolved in the wastewater, resulting in an insoluble metal phosphate that settles out through sedimentation. Calcium (Ca), aluminium (Al) and iron (Fe) are commonly used for the dosing of metal ions, and these are added as chlorides or sulfates (Metcalf and Eddy 2003). Commonly used iron coagulants include ferric sulfate, ferrous sulfate and ferric chloride whereas ammonium coagulants include aluminium sulfate, and aluminium chloride (Water Environment Federation, 2011).

Chemical dosing is typically done as a part of the tertiary treatment process. Chemical P removal has several advantages over biological P removal, including being less sensitive to changes in influent characteristics, loading rate, and temperature.

Furthermore, the chemical treatment takes less time to complete, as opposed to biological P removal, where performance gradually improves over time due to microbial growth. Chemical addition in tertiary treatment results in high-quality effluent and leads to high chemical cost and the production of additional chemical tertiary sludge (Sengupta et al., 2015). During chemical coagulation, the phase change of dissolved phosphorus into particulate matter occurs, allowing for easy separation from the liquid. The desired metal compound can be precipitated under supersaturated conditions, which could be accomplished by a pH change, an increase in metal ion concentration, or a combination of the two (Le Corre et al., 2009).

Chemical struvite precipitation has been applied both in the laboratory scale and the commercial scale. The struvite precipitation requires modifications of process parameters due to variations in the characteristics of the wastewater. The addition of an external magnesium source to provide a molar ratio of Mg, phosphorus, and nitrogen to promote struvite precipitation is involved in this process. Moreover, struvite precipitation also requires alkaline pH for struvite precipitation. Mg is typically added in the form of magnesium salts such as  $MgCl_2$ ,  $MgSO_4$ , and  $MgO$ . Additionally, alkaline pH is required for struvite precipitation (Kataki et al., 2016).

### 2.3.3 Biological Phosphorus Removal

Biological P removal is based upon the principle of phosphorus accumulation from the wastewater into the biomass of the phosphorus accumulating organisms (PAOs), allowing this P to be removed and applied directly (as sludge) to agricultural land, or solubilized and recovered as a mineral product, such as struvite (Oluwafeyikemi, 2013).

PAOs store phosphate as polyphosphate under aerobic conditions, using up polyhydroxybutyrate (PHB) as organic carbon.

The process of improving the storage capacity of P as polyphosphate by PAOs biomass in activated sludge is known as Enhanced Biological Phosphorus Removal (EBPR). EBPR operates on the principle that some organisms can take up more P than they need for cellular growth, a phenomenon known as "luxury uptake." There are several types of PAOs that can take up P in excess amounts as energy-rich polyphosphates, with P content ranging from 20-30% of dry weight, whereas common heterotrophic bacteria have a P content of about 2% (Metcalf and Eddy 2014). In the biological method, phosphorus can be recovered in two forms, i.e., biomass and mineral form. Phosphorus is concentrated in sludge in biomass form and can be recovered for agricultural use, whereas struvite recovery takes place in mineral form for commercial fertilizer or industrial application.

This method can be useful for accumulating up to 90% of the phosphorus in the sludge under optimal conditions. This method produces lower sludge compared to chemical precipitation due to lack of chemical usage (Morse et al., 1998). When compared to chemical coagulation, this process reduces both the chemical cost and volume of the sludge generated. However, this process involves more complex configuration and operating regimes and high energy consumption (Ning *et al.*, 2008; Peleka and Deliyanni, 2009). This method also requires the addition of readily biodegradable organic carbon. Furthermore, temperature and feed concentrations have an impact on the performance of the microorganism (Oehmen *et al.*, 2007).

#### 2.3.4 Adsorption

Adsorption refers to the accumulation of solute molecules (adsorbate) on the solid surface (adsorbent). It can occur because of the physical or chemical properties of the adsorbent and/or adsorbate. For physical adsorption, van der Waals forces attract the targeted solute, whereas chemical adsorption uses chemical reactions to remove the targeted solute. Phosphorus is removed from the wastewater effluent until the adsorbents are completely exhausted. After that, the saturated adsorption media are then removed and regenerated, allowing P to be recovered as a concentrated stream. The adsorption media can be regenerated through a variety of methods, which include washing with nitric acid ( $\text{HNO}_3$ ) or sodium chloride ( $\text{NaCl}$ ), as well as biological regeneration (Vaneckhaute et al., 2017).

Selection of technique depends on the type of adsorbent media. No additional sludge formations take place as this method employs physical force between adsorbate and adsorbent. This method required little maintenance except for cleaning, regeneration, and removal of phosphorus from regenerant. The efficiency of removal of phosphorus using this method is very low. Maximum P removal of 18% has been reported for the treatment of human urine using clinoptilolite at the laboratory scale. This method has several limitations including fouling of the adsorbent bed, as well as maintaining bed capacity after multiple regeneration cycles, the high cost of regenerant solutions and sorbents, as well as the safe disposal of spent regenerant (Sengupta et al., 2015).

## 2.4 Electrocoagulation Principles

Electrocoagulation is an emerging technology alternative to chemical coagulation for treatment of wastewater. This method involves coagulation along with flotation for the removal of dissolved and suspended contaminants. The electrode arrangement in electrocoagulation reactor can be composed of two electrodes (one cathode and one anode) or many electrodes. During electrocoagulation, metal ions are generated from the anode under the application of electric current. These metal ions ( $M^{z+}$ ) react with the phosphate ions present in the solution resulting in the formation of insoluble precipitates (Huang et al., 2017). Formation of metal hydroxide and polyhydroxides compounds takes place which causes destabilization and aggregation of colloidal substances. The generation of hydrogen at the cathode propels flocs to the water surface by adding buoyancy (Figure 1).

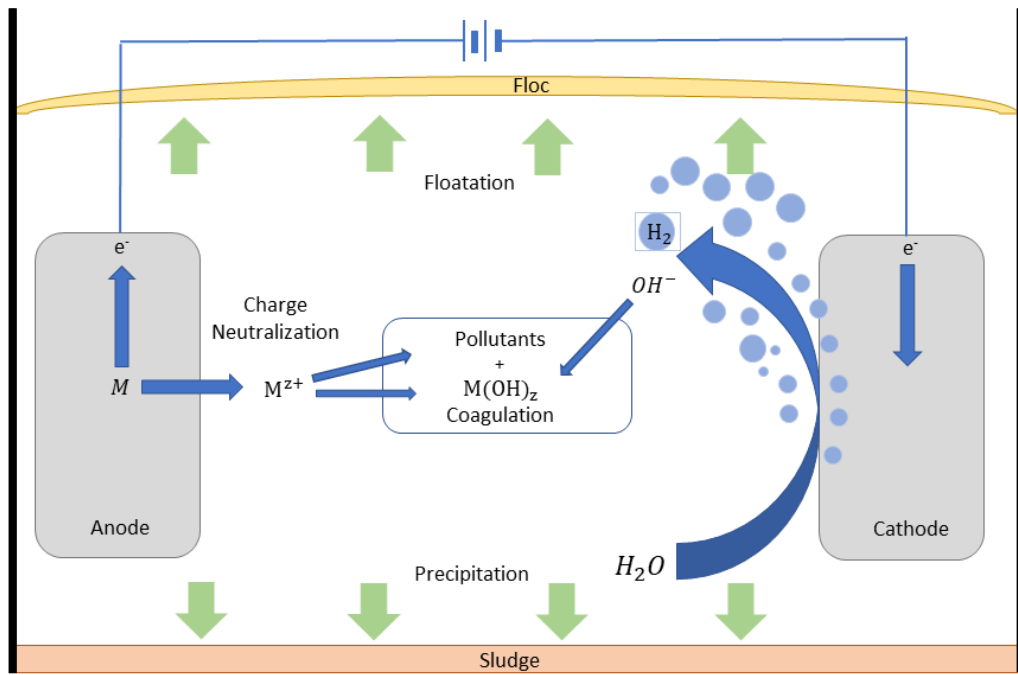
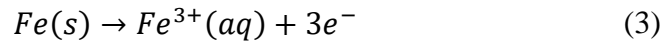
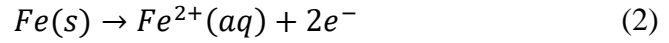


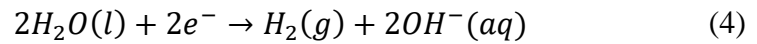
**Figure 1: Mechanism of electrocoagulation**

The dominant reactions for iron as an electrode material are as follows (Bernal-Martínez et al., 2013; Linares-Hernández et al., 2010) :

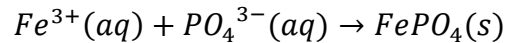
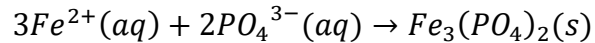
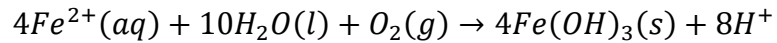
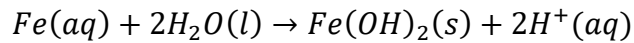
Anode Reaction:



Cathode Reaction:



Formation of compounds such as  $Fe_3(PO_4)_2$ ,  $Fe(OH)_2$  and  $Fe(OH)_3$  can take place in the bulk solution according to the following reactions.

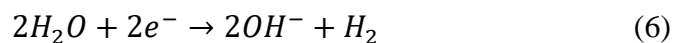


The dominant reactions for magnesium as an electrode material for the electrochemical struvite precipitation are as follows:

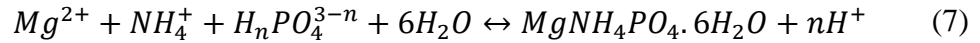
Anode Reaction:



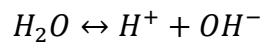
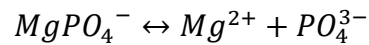
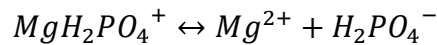
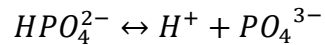
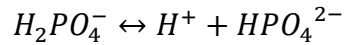
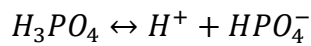
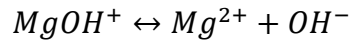
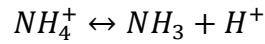
Cathode Reaction:



The general equation for struvite formation is as shown in equation 3.



Other chemical reactions taking place during struvite formation are described below (Doyle & Parsons, 2002).



#### 2.4.1 Advantages of Electrocoagulation

The benefits of electrocoagulation process over other available methods are listed below (Mollah et al., 2001).

- This method involves simple reactor configuration and easy operation.
- This process does not involve addition of chemical coagulants and produces less sludge compared to chemical coagulation. The sludge from this process tends to settle more easily than that of chemical coagulation.

- This process is efficient for removal of small colloidal particles. The generation of hydrogen at the cathode propels flocs to the water surface.
- Because there are few moving parts in this configuration, it requires less maintenance.
- This system can be powered by solar energy, making it feasible for rural communities to install.

#### 2.4.2 Disadvantages of Electrocoagulation

The drawbacks of electrocoagulation process are listed below (Mollah et al., 2001).

- The sacrificial electrodes are the consumable component that must be replaced on regular basis.
- This method necessitates the availability of electricity. In some areas, the cost of electricity may be prohibitively high.
- Electrode passivation occurs, resulting in decreased efficiency and high energy consumption.
- The conductivity of the wastewater should be sufficient for electrocoagulation. The energy requirement is entirely dependent on the conductivity of the wastewater.

Most of the disadvantages of this process can be mitigated at the local level. The suggested methods for mitigating the aforementioned issues are listed below.

The electrodes can be sourced locally. Iron and aluminium electrodes are cheap compared to magnesium electrodes. Power consumption can be reduced by optimizing

the electrocoagulation process variables. Furthermore, depending upon the volume of the wastewater, solar energy can be used to power this system. Electrode passivation can be reduced by reversing the electrode polarity; otherwise, mechanical cleaning is required.

### 2.4.3 Electrodes Arrangement

The electrode arrangement influences the efficiency of electrocoagulation. The arrangement can be composed of two electrodes (one cathode and one anode), or it can be made up of many electrodes. The complex configuration of electrodes increases the sacrificial surface area, resulting in faster metal ion addition. The electrode configurations can be divided into the following categories (Hakizimana et al., 2017).

- a) Monopolar Parallel: This arrangement consists of cathodes and anodes placed alternatively in parallel. The electrodes are then connected to the respective terminal for power supply as shown in Figure 2(a).
- b) Monopolar Series: In this configuration, the outermost electrodes (one cathode and one anode) are connected to the power source. Inner electrodes are connected together but they are not connected to the power supply as shown in Figure 2(b).
- c) Bipolar Series: In this configuration, the outermost electrodes are connected to a power supply. Inner electrodes work on the principle of charge polarization. The outer electrodes function as monopolar electrodes whereas the inner electrodes function as bipolar electrodes.

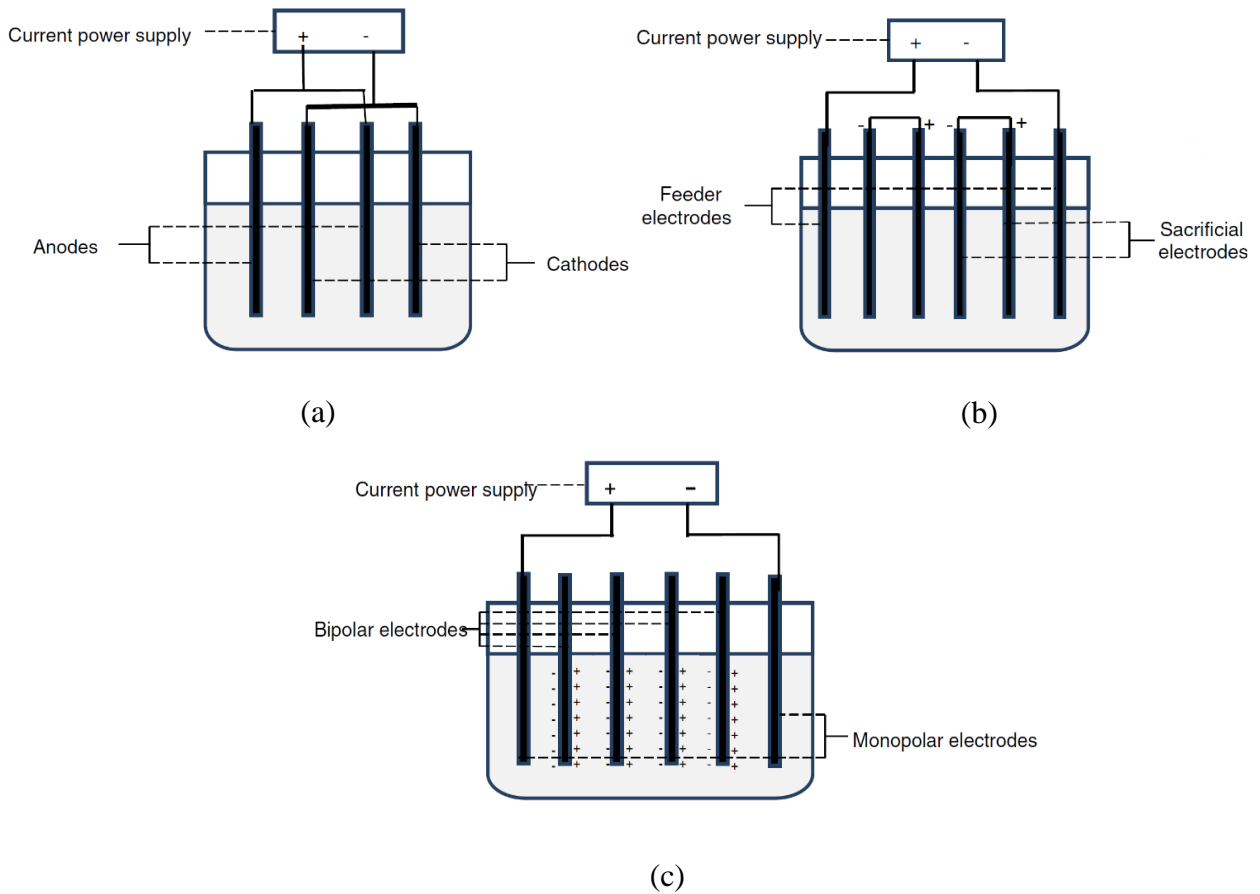


**Figure 2: Electrodes arrangement: (a) Monopolar parallel (b) Monopolar series (c) Bipolar in series (Hakizimana et al., 2017)**

The selection of electrode arrangement is determined by the volume of the wastewater treated and the mode of operation of the reactor. A monopolar electrode configuration is found to be more energy efficient than bipolar electrodes, lowering the cost of operation (Asselin et al., 2008; Sahu et al., 2014). However, the bipolar mode performs better in terms of contaminant removal and has the advantage of being simple to configure (Ghosh et al., 2008; Jiang et al., 2002).

## 2.5 Factors affecting Electrocoagulation

Phosphorus removal and recovery using the electrocoagulation method are influenced by several physicochemical factors including pH, retention time, current density, and inter-electrode distance.

### 2.5.1 Initial pH

The initial pH of the solution is a critical factor for the removal and recovery of total phosphorus from wastewater. It influences the mechanism of pollutant removal during the electrocoagulation process. It affects the conductivity of the solution and the dissolution of the anode. In acidic and alkaline conditions, the reactions of electrode dissolution change due to the formation of various hydroxides. For amphoteric electrode materials such as iron and aluminum, formation of various hydroxide compounds takes place depending upon the solution pH (Sasson et al., 2009). The charge of different hydroxides affects their oxidation potential and thus their ability to coagulate.

For iron as an electrode material, formation of effective coagulant species takes place in acidic pH whereas formation of  $\text{Fe}(\text{OH})_4^-$  ion takes place in alkaline condition. Because of the formation of  $\text{OH}^-$  ions in the cathode during the electrocoagulation process, the pH of the solution rises. Even without electricity, the addition of Fe ions into the solution by anodic dissolution was found to be significant for acidic pH. Furthermore, when the pH rises above 5, ferrous ions oxidise to ferric ions (Sasson et al., 2009). Anodic dissolution decreases with alkaline pH as anode corrosion decreases due to electrode passivation. It has been suggested that initial pH is a key parameter when either chemical

coagulation or EC is selected for the water treatment (Nasr et al., 2019). However, the optimal pH value varies depending on the pollutant to be removed from wastewater.

During electrochemical struvite crystallisation,  $H^+$  ions are released into the solution according to equation (7), lowering the pH. The rate of the pH change affects the formation of struvite particles as well as the quality of the crystals formed (Le Corre et al., 2009). According to Ohlinger et al. (1998), the solubility of struvite decreases with an increasing pH within the pH range of 6 to 8. The identified pH value associated with minimum solubility ranges from pH 8 to 10.7 (Booker et al., 1999; Ohlinger et al., 1998). Increasing the initial pH of the solution causes an increase in supersaturation thereby leading to the formation of struvite crystals and crystal growth (Le Corre, 2006). Furthermore, high initial pH causes the formation of ammonia gas from an aqueous solution, resulting in a decrease in ammonia ion concentration and, as a result, affecting the formation of struvite (Stumm & Morgan, 1996).

### 2.5.2 Retention Time

Retention time is defined as the duration of electrodes in contact with the wastewater under the application of electric current. It affects the effectiveness of electrocoagulation because it controls the duration of metal ion addition from the anode. For a constant current density, increase in retention time leads to the formation of more metal ions into the solution thereby increasing floc formation and removal efficiency (Khandegar & Saroha, 2013). This can be explained using Faraday's Law. After the optimal retention time has been reached, a sufficient amount of metal ions (coagulant) will be added to promote floc formation. Extending the retention time

beyond the optimal value can result in increased energy consumption while having no effect on pollutant removal.

### 2.5.3 Current Density

The current density has a significant impact on the rate of electrocoagulation process (Bektas et al., 2004). It influences the rate of coagulant production and the formation of bubbles. Current density is defined as the applied electric current per unit area of the active surface of a sacrificial electrode. An increase in current density causes an increase in the production of metal ions (coagulant), resulting in higher phosphorus recovery. Furthermore, as current density increases, the rate of bubble formation increases while the size of the bubble decreases. Both effects are advantageous for high pollutant removal via H<sub>2</sub> flotation (Holt et al., 2002; Kobya et al., 2006). The rate of production of metal ions by the anodic dissolution can be calculated using the Faraday's law as shown in equation 8.

$$m = \frac{ItM}{zF} \quad (8)$$

The concentration of metal ions can be calculated as follows

$$C = \frac{m}{V} = \frac{ItM}{zFV} \quad (9)$$

Here, C represents the concentration of the metal ion m represents the mass of the metal generated, I represents the current, t represents the treatment time, M represents the material's molar mass, z represents the valency of the produced ion, F represents the Faraday's constant (96500 C/mol), and V represents the reactor volume. However, this equation does not consider electrode surface conditions. In the case of electrode passivation, the rate of generation would be much smaller (Khemis et al., 2005). The

ideal current density should be high enough to produce enough coagulant for pollutant removal but not excessive, as this would result in high energy consumption.

#### 2.5.4 Inter-electrode Distance

Inter-electrode distance is defined as the distance between the electrodes. It is an important factor affecting the performance of electrocoagulation system. According to Attour et al. (2014), inter-electrode distance is directly proportional to the resistivity of the solution and indirectly proportional to the conductivity of the solution. Furthermore, increasing the inter-electrode distance leads to an increase in cell voltage and, as a result, higher power consumption (Calvo et al., 2003). Nasrullah et al. (2019) discovered that increasing the inter-electrode distance increases resistance because of increased water flow between electrodes and decreases electron transfer, thereby affecting electrocoagulation performance. An inter-electrode distance within the range of 0.5 cm to 1.5 cm results in the formation of flocs larger than 2 cm, which have the ability to adsorb more contaminants, thereby increasing removal efficiency (Nasrullah et al., 2019). The optimal inter-electrode distance should strike a balance between reducing energy consumption by decreasing the inter-electrode distance while still allowing for larger floc formation (Sahu et al., 2014).

#### 2.6 Response Surface Methodology

Response surface methodology is a statistical tool for optimizing the responses when two or more quantitative factors are involved. The dependent variables are called responses and independent variables, or factors are called predictor variables. It is

extremely useful for optimizing variables/factors in a more practical manner. This optimization technique employs statistical techniques to fit the experimental data into a polynomial equation. The polynomial equation acts as a predictive model which describes the behaviour of a given set of data in order to make statistical predictions (Bezzera et al., 2008). It is useful when a response or set of responses of interest is influenced by a number of variables. The goal is to optimise the levels of these variables at the same time in order to achieve the best system performance. To achieve this goal, linear or square polynomial functions are used to describe the system under consideration and, as a result, to model the experiments until optimal conditions are achieved. (Bezzera et al., 2008). RSM analysis is based on the assumption that a response (Y) is a mathematical function of variables  $(x_1, x_2, x_3 \dots, x_k)$ . RSM commonly uses first-order and second-order polynomial models.

First-Order polynomial:

$$Y = \beta_0 + \sum_{i=1}^k \beta_i x_i + \varepsilon \quad (10)$$

Second-Order Polynomial:

$$Y = \beta_0 + \sum_{i=1}^k \beta_i x_i + \sum_{i < j} \beta_{ij} x_i x_j + \sum_{i=1}^k \beta_{ii} x_i^2 + \varepsilon \quad (11)$$

Here, k represents the number of variables,  $\beta_0$  is the constant term,  $\beta_i$  represents the coefficients of the linear parameters,  $x_i$  represents the variables, and  $\varepsilon$  is the residual associated with the experiments. In order to estimate the parameters, the experimental design should include a minimum of three levels of the factor. For first-order, the most

common design is  $2^k$  factorial design, followed by the Plackett-Burman design, and for second-order, central composite design and Box-Behnken design (Montgomery, 1999). The second-order (quadratic) model is useful for identifying curvature in the response, which leads to better mapping of the response surface. This experimental design overcomes the limitations of traditional optimization such as optimizing one variable at a time (OVAT). RSM involves the simultaneous optimization of predictor variables resulting in fewer experiments (Rout et al., 2014).

### 2.6.1 Central Composite Design

Central composite design uses a second-order polynomial model. It was developed by Box and Wilson in 1951. This experimental design is useful to maximize, minimize or reach a specific target for the value of a response variable. It consists of full factorial points, star points (axial), and center points. Center points indicate whether curvature exists in the system. If discovered, the addition of star points allows for the estimation of pure quadratic terms. Two levels of the variable contribute significantly to the estimation of the effect of linear terms and two-factor interactions. In this case, factorial points help estimate interaction terms, while axial points help estimate quadratic terms. The central points contribute to the estimation of error as well as quadratic terms (Kuehl, 2000). The central composite design provides significant flexibility in the selection of axial distance ( $\alpha$ ) and number of central runs ( $C_0$ ) which is very important. Figure 3 depicts the central composite design with two factors ( $k=2$ ) and three factors ( $k=3$ ). The axial distance ( $\alpha$ ) will be  $\sqrt{2}$  and  $\sqrt{3}$  for  $k$  values of 2 and 3 respectively. The design

includes 8 circumscribed points and a central run for 2 variables, and 14 points on a spherical surface and central runs for 3 variables.

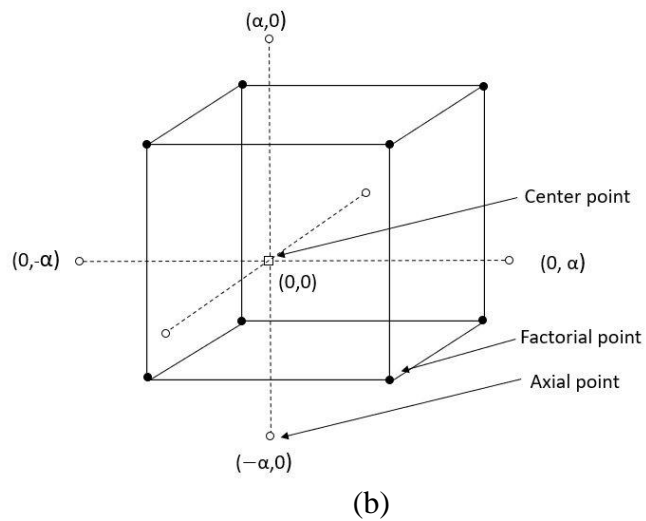
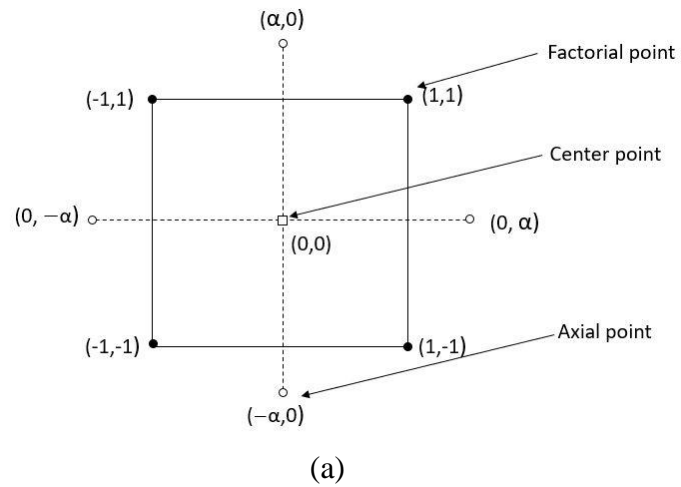


**Figure 3: Central composite design: (a) Two variables ( $k = 2$ ) (b) Three variables ( $k = 3$ )  
(Bezerra et al., 2008)**

### 3. Materials and Methods

#### 3.1 Anaerobic Bioreactor Effluent and Characteristics

Anaerobic bioreactor effluent and digestate was collected from an industrial wastewater treatment plant (McCain Foods, Florenceville-Bristol, Canada). The WWTP uses a large covered anaerobic lagoon for the treatment of its wastewater and to generate biogas. The collected sample was stored in a refrigerator under 2° C to avoid degradation of organic matter present in it. The collected anaerobic bioreactor effluent and digestate was homogenized for initial characterization. The physicochemical characteristics of the anaerobic bioreactor effluent are shown in Table 2. The analysis to characterize the effluent was performed in triplicate.

**Table 2: Characteristics of anaerobic effluent**

Parameter	Unit	Value
pH	-	7.5 ± 0.25
Conductivity	mS/cm	2.7 ± 0.09
COD	mg/L	323.7 ± 8.5
fCOD	mg/L	119.1. ± 5
TP	mg/L	45.6 ± 2
NH <sub>3</sub> -N	mg/L	160 ± 2.5
Ca	mg/L	70.9 ± 2
Mg	mg/L	12± 0.5
Na	mg/L	96.4 ± 3

#### 3.2 Experimental Setup and Operation

The reaction was carried out in a batch reactor, with a working volume of 1 litre. Iron and magnesium electrodes were used, having an active surface area of 20 cm<sup>2</sup> each

having dimensions of width, 4 cm; height, 5 cm; and thickness, 0.2 cm. Two electrodes were connected to a DC power supply which had a variable output of 0-120 V. A schematic of the experimental setup is presented in Figure 4. The formation of the metal oxides was observed on the surface of the anode after each run. This is referred to as electrode passivation, and it results in increased electricity consumption. The electrodes were scraped after each run using abrasive paper followed by rinsing them several times with distilled water. All experiments were carried out at room temperature (22<sup>o</sup> C).

Anaerobic bioreactor effluent was filtered through glass fiber filters (Whatman, 47 mm) with a pore size of 1.2  $\mu\text{m}$  to eliminate the effects of suspended solids in the experiment. During each run, samples of 10 mL were collected from the surface at an interval of 2.5 minutes and filtered through cellulose acetate membrane filters (Whatman, 47 mm) with a pore size of 0.45  $\mu\text{m}$ . Constant stirring was done using a magnetic stirrer. The filtrate was acidified using ACS-grade nitric acid for elemental analysis. Electrocoagulation effluent was centrifuged to separate flocs and precipitate from the treated effluent. This precipitate from the iron EC reactor was oven dried at 105<sup>o</sup>C, while the precipitate from the magnesium EC reactor was dried at room temperature for X-ray diffraction (XRD), energy dispersive spectroscopy (EDS), and scanning electron microscopy (SEM). Following the combustion of the iron EC sludge at 900<sup>o</sup>C, acid leaching tests were carried out at a fixed acid load of 100 kg/kg P and different liquid-to-solid (L/S) ratios (50 mL/g, 100 mL/g, 150 mL/g, and 200 mL/g) to find the optimum L/S ratio for maximum phosphorus extraction. Acid leaching was carried out in a closed conical flask. A magnetic stirrer was used to constantly stir the acid and

sludge ash mixture present inside the flask. Samples were collected after a contact time of 24 hours and filtered through cellulose acetate membrane for elemental analysis.

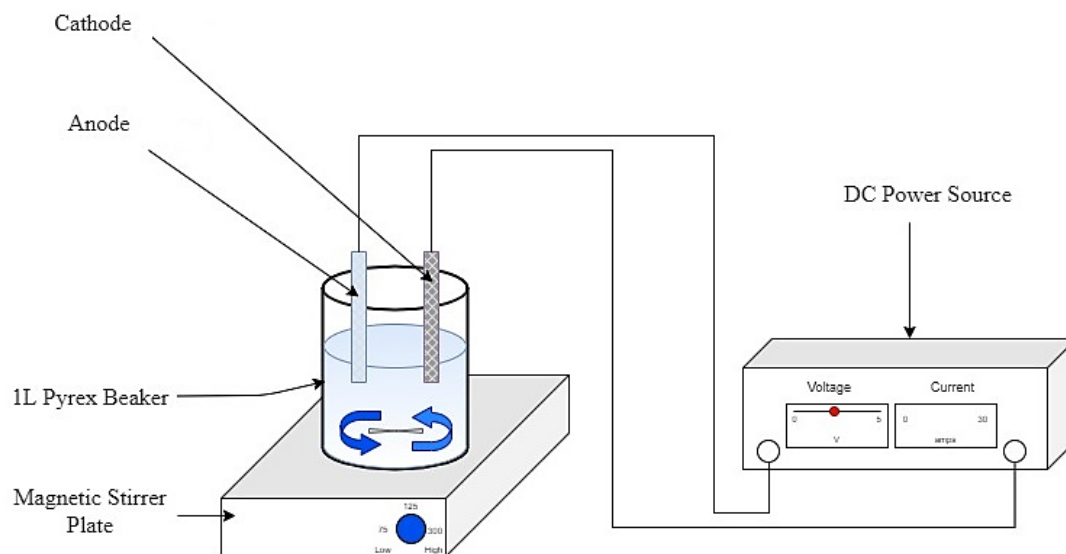


**Figure 4: Schematic of the EC batch reactor setup**

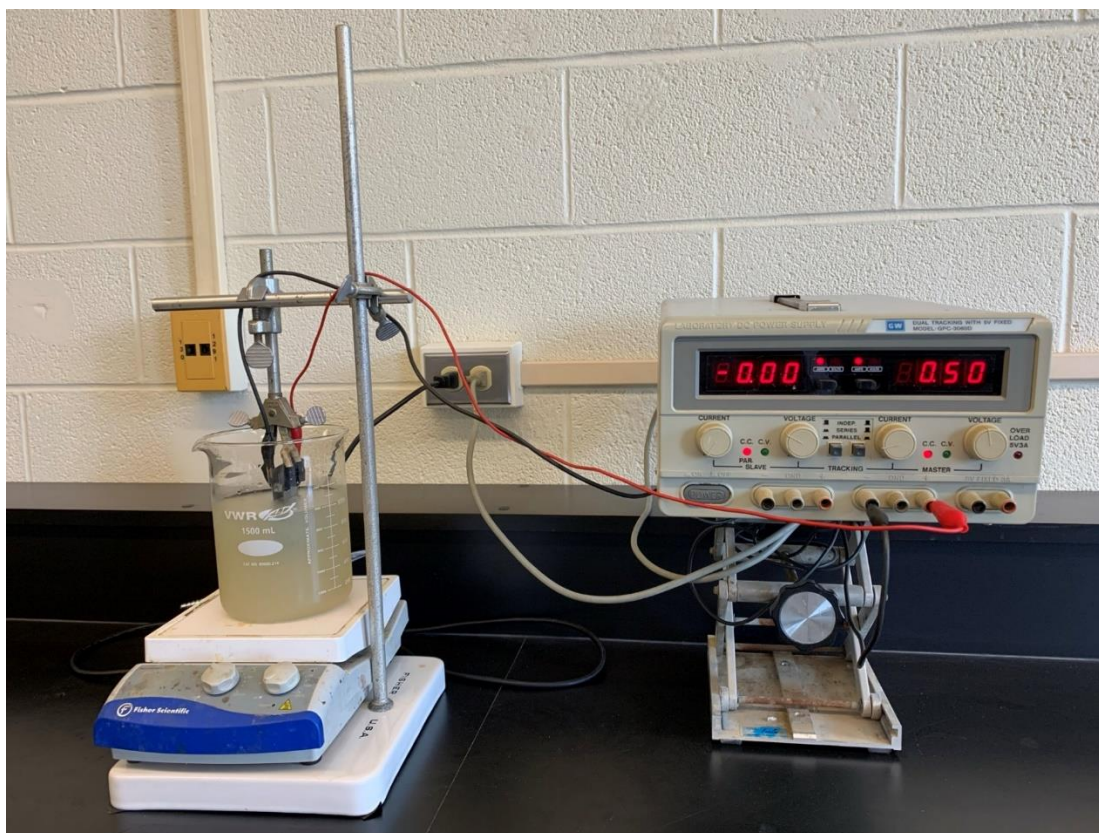


**Figure 5: Photograph of the EC batch reactor setup**

### 3.3 Development of Central Composite Design

In this study full factorial central composite design (CCD) with Five levels (-2, -1, 0, 1, 2) was used to evaluate the significant impacts of the independent variables and their interaction on the dependent variables. Tables 3 and 4 present the independent variables and levels as defined by the CCD design. For this study, TP removal efficiency was chosen as the response. The ranges of the independent process variables were determined by preliminary studies. The number of experiments needed for this study was determined by Equation (12) as follows:

$$N = 2^K + 2K + C_0 \quad (12)$$

Where N is the number of experiments, K is the number of factors, and  $C_0$  is the number of central points. The experimental design for 4 factors with 7 central points involves 31 experimental runs. The independent process variables for this study are initial pH (pH), retention time (RT), current density (CD) and inter-electrode distance (IED). For this study, TP removal efficiency was chosen as the response. In this study, a central composite design (CCD) was chosen and MiniTab statistical analysis software was used to create the model. A full factorial central composite design was selected as this study involves 5-level independent variables.

**Table 3: Independent variables and levels: Iron EC runs**

Variables	-2( $\alpha$ )	-1	0	+1	+2( $\alpha$ )
pH	3	4.75	6.5	8.25	10
Retention Time (min)	5	7.5	10	12.5	15
Current Density (A/m <sup>2</sup> )	100	150	200	250	300
Inter-electrode Distance (cm)	0.5	0.75	1	1.25	1.5

**Table 4: Independent variables and levels: Magnesium EC runs**

Variables	-2( $\alpha$ )	-1	0	+1	+2( $\alpha$ )
pH	6.5	7.5	8.5	9.5	10.5
Retention Time (min)	15	20	25	30	35
Current Density (A/m <sup>2</sup> )	100	150	200	250	300
Inter-electrode Distance (cm)	0.5	0.75	1	1.25	1.5

### 3.4 Analytical Methods

Analytical methods used during the study are described below in accordance with Standard Methods (APHA, AWWA, and WEF 2005).

#### 3.4.1 Total Phosphorus (TP)

Analysis of total phosphorus was carried out using ICP-OES with standardized solution concentrations of 1 mg/L, 2 mg/L and 10mg/L.

#### 3.4.2 Chemical Oxygen Demand (COD)

Chemical Oxygen Demand (COD) is an indicator of the level of pollution in wastewater. It is a measurement of the amount of oxygen required to degrade organic matter present in a given sample.

Filtered COD (fCOD): Filtered COD was determined by measuring the filtrate after filtering the water sample through the glass fiber filter (Whatman, 47mm) of a pore size of 1.2  $\mu$ m.

#### 3.4.4 pH

The pH of the water samples was measured using a digital pH meter (AB15, Fisher Scientific, USA). The pH probe was calibrated with standardized pH solutions of pH 4.0, 7.0 and 10.0.

### 3.4.5 Ammonia-Nitrogen (NH<sub>3</sub>-N)

NH<sub>3</sub>-N concentration was measured using HACH UV-Spectrophotometer (DR 2700, HACH, USA). Salicylate method was followed (range 0.4 to 50.0 mg/L) for measurement of NH<sub>3</sub>-N using ammonia salicylate and ammonium cyanurate reagent powder pillows.

### 3.4.6 XRD Analysis

X-ray powder patterns for all the samples were measured using a Bruker D8 advance spectrometer. The X-ray source was a sealed, 2.2kW Cu X-ray tube, maintained at an operating current of 40 kV and 25 mA. The analysis was carried out on powdered precipitate.

### 3.4.7 SEM Analysis

Analysis was performed with a JEOL JSM-6400 Scanning Electron Microscope equipped with an EDAX Genesis 4000 Energy Dispersive X-ray (EDS) analyser. Samples were carbon coated using an Edwards 306A carbon coater before observation in the microscope.

### 3.4.8 Data Collection

The variables and their frequency of measurement are presented in Table 5.

**Table 5: Data collection frequency**

<b>Variables</b>	<b>Data Collection Frequency</b>
TP concentration	3 times a week
NH <sub>3</sub> -N	3 times a week
pH	5 times a week
fCOD	3 times a week
XRD	3 times a month
SEM	once a month

### 3.4.9 Data Analysis

Total phosphorus (TP) and fCOD concentrations were measured in samples collected from the iron electrocoagulation system, while TP, fCOD, and NH<sub>3</sub>-N were measured in samples collected from the magnesium electrocoagulation system. The removal efficiency of these parameters was calculated using Equation (13).

$$\text{Removal Efficiency (\%)} = \frac{C_i - C_f}{C_i} \times 100 \quad (13)$$

Here C<sub>i</sub> and C<sub>f</sub> are the initial and final concentrations of the parameter.

Energy consumption is critical in electrochemical processes because electricity is the energy source. This is a parameter used to determine the process's applicability. Energy consumption under optimal conditions was determined by the following equation.

$$\text{Energy Consumption} \left( KW \cdot \frac{h}{m^3} \right) = \frac{E \times I \times t}{V \times 1000} \quad (14)$$

Here E denotes the voltage, I denotes the current applied, t denotes the retention time in hours and V denotes the volume of the effluent treated in m<sup>3</sup>.

### 3.4.10 Quality Control

The water samples for elemental analysis were filtered through 0.45 μm cellulose acetate membrane and pretreated with 5% HNO<sub>3</sub>. These samples were stored in a refrigerator. TP concentration was measured in triplicate using ICP-OES. All the electrocoagulation experiments were conducted in duplicates, and the results demonstrated good repeatability. COD analysis of the filtered electrocoagulation

effluents was carried out in triplicates.  $\text{NH}_3\text{-N}$  concentration of the samples were measured in duplicates. Instruments were calibrated on a regular basis to ensure the reliability of the results.

### 3.5 Optimization

Response optimization tool in Minitab software (version 20) was used to maximize the TP recovery efficiency. This function is used to identify the level of variables in order to maximize, minimize or to attain a specific target of the response. It is useful to evaluate the impact of multiple variables on a response. It combines the levels of the variables to optimize the response variable. This study focuses on a single response i.e., TP recovery. The experimental data were fitted to a quadratic model in order to use the response optimizer function. Experiments were carried out under optimized conditions to validate the quadratic model.

## 4. Results and Discussion

This chapter describes the response surface design results, including the analysis of variance (ANOVA), as well as the response surface and contour plots. For the iron-electrocoagulation system, the effect of independent process variables on TP removal and COD removal was discussed. Parameters such as TP recovery, COD removal, and ammonium nitrogen removal were discussed for the magnesium electrocoagulation system.

### 4.1 Iron Electrocoagulation System

Thirty-one experimental runs were carried out as per central composite design (CCD), for modelling the TP removal. The independent process variables for this study are initial pH (pH), retention time (RT), current density (CD) and inter-electrode distance (IED).

Table 6 lists the design matrix and run parameters as per central composite design.

**Table 6: Design matrix: Iron EC runs**

Run Order	Coded Variables				TP Removal Efficiency (%)	
	pH	RT	CD	IED	Experimental	Predicted
1	-1	-1	-1	-1	7.47	8.76
2	1	-1	-1	-1	72.825	72.64
3	-1	1	-1	-1	36.08	37.91
4	1	1	-1	-1	91.28	93.04
5	-1	-1	1	-1	34.58	37.47
6	1	-1	1	-1	84.07	80.15
7	-1	1	1	-1	67.43	66.61
8	1	1	1	-1	96.94	100.55
9	-1	-1	-1	1	27.09	22.97
10	1	-1	-1	1	71.5	73.31
11	-1	1	-1	1	36.08	40.58

**Table 6: Design matrix: Iron EC runs (Continued)**

12	1	1	-1	1	86	82.19
13	-1	-1	1	1	61.69	60.51
14	1	-1	1	1	92.41	89.66
15	-1	1	1	1	78.45	78.13
16	1	1	1	1	98.83	98.54
17	-2	0	0	0	5.4	3.41
18	2	0	0	0	85.77	87.69
19	0	-2	0	0	42.06	45.18
20	0	2	0	0	86.4	83.21
21	0	0	-2	0	49.23	47.73
22	0	0	2	0	91.35	92.78
23	0	0	0	-2	76.51	74.66
24	0	0	0	2	82.39	86.85
25	0	0	0	0	77.38	80.76
26	0	0	0	0	80.13	80.76
27	0	0	0	0	81.71	80.76
28	0	0	0	0	79.96	80.76
29	0	0	0	0	85.69	80.76
30	0	0	0	0	80.65	80.76
31	0	0	0	0	82.47	80.76

#### 4.1.1 Statistical Analysis

Analysis of Variance (ANOVA) was used to assess the significance of the quadratic model for predicting TP removal efficiency. The model summary is shown in Table 7. The results obtained from the ANOVA are represented in Table 8. The significance of model terms was evaluated using p-value. A p-value of less than 0.05 indicates that the independent variable has a significant influence on the response. The results showed that 12 out of the 14 model terms were found to be significant for total phosphorus (TP) removal efficiency. This includes the linear terms such as pH (A), RT (B), CD (C) and IED (D), as well

as squared terms such as pH<sup>2</sup> (A<sup>2</sup>), RT<sup>2</sup> (B<sup>2</sup>), CD<sup>2</sup>(C<sup>2</sup>), and interaction terms such as pH · RT (AB), pH · CD (AC), pH · IED (AD), RT · IED (BD), CD · IED (CD).

**Table 7: Model summary: Iron EC runs**

Parameter	R <sup>2</sup> (%)	Adjusted R <sup>2</sup> (%)	Predicted R <sup>2</sup> (%)	P <sub>lof</sub>
Total Phosphorus	98.96	98.27	96.27	0.142

\*lof-lack of fit

**Table 8: ANOVA results: Iron EC runs**

Source	DF	Adj SS	Adj MS	F-Value	P-Value	Remarks
Model	14	19639.7	1402.8	111.40	0.000	Significant
Linear	4	16092.6	4023.1	319.47	0.000	Significant
A	1	10656.6	10656.6	846.22	0.000	Significant
B	1	2168.6	2168.6	172.20	0.000	Significant
C	1	3044.6	3044.6	241.77	0.000	Significant
D	1	222.9	222.9	17.70	0.001	Significant
Square	4	2627.2	656.8	52.16	0.000	Significant
A*A	1	2235.7	2235.7	177.54	0.000	Significant
B*B	1	499.9	499.9	39.69	0.000	Significant
C*C	1	203.2	203.2	16.14	0.001	Significant
D*D	1	4.0	4.0	0.32	0.579	Not significant
2-Way Interaction	6	919.9	153.3	12.18	0.000	Significant
A*B	1	76.4	76.4	6.07	0.025	Significant
A*C	1	449.3	449.3	35.68	0.000	Significant
A*D	1	183.1	183.1	14.54	0.002	Significant
B*C	1	0.2	0.2	0.01	0.909	Not significant
B*D	1	132.9	132.9	10.55	0.005	Significant
C*D	1	78.1	78.1	6.20	0.024	Significant
Error	16	201.5	12.6	-	-	-
Lack-of-Fit	10	161.9	16.2	2.45	0.142	Not significant
Pure Error	6	39.6	6.6	-	-	-
Total	30	19841.2	-	-	-	-

The lack-of-fit test for the TP removal efficiency (p-value = 0.142) was found to be nonsignificant. A high R<sup>2</sup> value signifies a good fit for the experimental data to the model.

R<sup>2</sup><sub>predicted</sub> value indicates the ability of the model to predict the response for a given set

of operating conditions. After the removal of statistically insignificant terms, the modified quadratic model for total phosphorus removal efficiency was obtained as equation (15).

**Total Phosphorus Removal Efficiency (%)**

$$\begin{aligned}
 &= 80.76 + 21.072 \text{ pH} + 9.506 \text{ RT} + 11.263 \text{ CD} + 3.047 \text{ IED} \\
 &- 8.802 \text{ pH}^2 - 4.141 \text{ RT}^2 - 2.626 \text{ CD}^2 - 2.185 \text{ pH} \cdot \text{RT} \\
 &- 5.299 \text{ pH} \cdot \text{CD} - 3.383 \text{ pH} \cdot \text{IED} - 2.882 \text{ RT} \cdot \text{IED} \quad (15) \\
 &+ 2.209 \text{ CD} \cdot \text{IED}
 \end{aligned}$$

According to ANOVA results, the coefficient of determination was found to be 0.99. It signifies that the statistical model can explain 99% of the variability in the response. In this study for the removal of total phosphorus, the  $R^2$  (0.99) value is fairly close to the adjusted  $R^2$  (0.98) and predicted  $R^2$  (0.96) values indicate that the model is valid (Makwana & Ahammed, 2017). Figure 6 presents the plot of observed vs predicted TP removal efficiency.

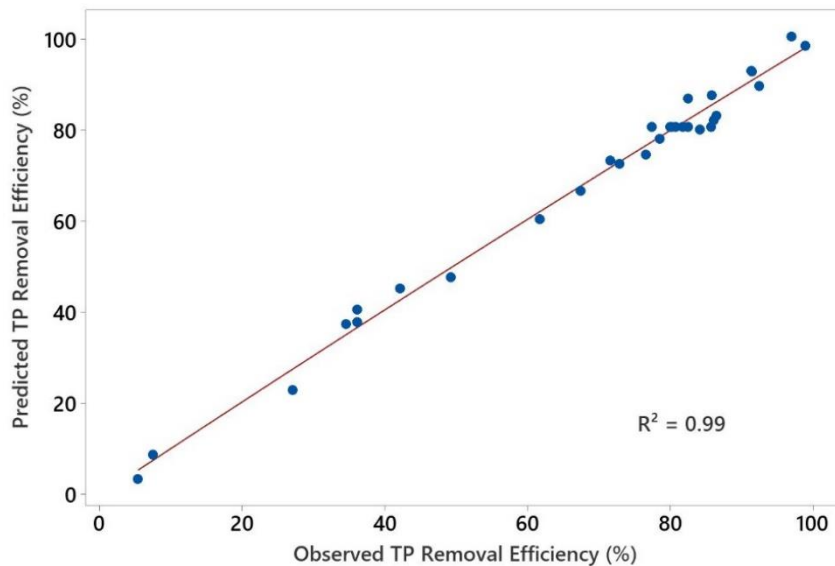


**Figure 6: Predicted vs Observed TP removal efficiency**

The model equation includes linear terms, quadratic terms, and interaction terms explaining the relationship of factors with the response variable. Initial pH was found to be the most important factor among linear and squared terms affecting total phosphorus (TP) removal. Interaction of initial pH and current density was found to be the most significant interaction term affecting the response. For the main effect (linear terms) in the quadratic model, a positive coefficient indicates that total phosphorus (TP) removal increases as the main effect increases, whereas a negative value would indicate that TP removal decreases as the main effect decreased.

#### 4.1.2 Effect of Independent Process Variables

##### 4.1.2.1 Initial pH (*pH*)

Total phosphorus removal efficiency was low under highly acidic conditions and gradually increased with increase in pH. It suggests that phosphorus removal mechanism for phosphorus removal is strongly influenced by the initial pH of the solution. Phosphate tends to precipitate as ferric phosphate ( $\text{FePO}_4$ ) at acidic pH due to lack of hydroxide ions ( $\text{OH}^-$ ). During electrocoagulation process, solution pH increases due to the formation of  $\text{OH}^-$  ions. Whereas at a higher pH range ( $>7$ ), the formation of ferric hydroxide ( $\text{Fe}(\text{OH})_3$ ) occurs. Ferric hydroxide acts as an adsorbent that provides active sites for the adsorption of phosphate (Sincero and Sincero 2003). Huang et al. (2017) found that phosphorus recovery from anaerobic bioreactor effluent using an iron-electrocoagulation system decreases as the initial pH increases, whereas Damaraju et al. (2020) reported that removal efficiency increases as the pH approaches neutral. However, interference of calcium ions in the iron electrocoagulation system for phosphorus removal has not been

observed so far. During the experiments, the formation of hydroxyapatite was observed under alkaline conditions ( $\text{pH} > 7.5$ ). In the current study, TP removal was found to be increasing with an increase in pH up to 9. Further increase in the initial pH of the solution leads to electrode passivation thereby causing a decrease in removal efficiency. Factorial plot for the initial pH is shown in Figure 7(a). Higher removal efficiency at alkaline pH can be ascribed to phosphorus adsorption by ferric hydroxide and the formation of calcium phosphate.

#### 4.1.2.2 Current Density (*CD*)

The current density has a significant impact on the rate of electrocoagulation process (Bektaş et al., 2004). According to Faraday's law, an increase in current density causes an increase in the production of metal ions (coagulant), resulting in higher phosphorus recovery. Furthermore, as current density increases, the rate of bubble formation increases while the size of the bubble decreases. Both effects are advantageous for high phosphorus removal via hydrogen flotation (Holt et al., 2002; Kobya et al., 2006). Within a current density range of  $100 \text{ A/m}^2$  to  $300 \text{ A/m}^2$ , phosphorus removal efficiency is found to increase with increasing current density. The factorial plot describes the relationship between the response and the predictor variable. It is a useful tool in response surface design because response surface design is efficient to provide more information with fewer experimental runs compared to the one variable at a time method. Factorial plot for current density is shown in Figure 7(b).

#### 4.1.2.3 Retention Time (*RT*)

TP removal efficiency is found to be increasing with an increase in retention time up to 12.5 minutes. For a given current density, the mass transfer from the anode into the solution in the form of metal ions is dependent on retention time. The extent of metal ion addition increases with an increase in retention time. According to the factorial plot for the retention shown in Figure 7(c), further increase in retention time beyond 12.5 minutes had a negligible effect on the removal efficiency because enough metal ions were already present in the solution. This observation is in agreement with findings by other researchers (Attour et al., 2014; Bakshi et al., 2020; Lacasa et al., 2011; Damaraju et al., 2020)

#### 4.1.2.4 Inter-electrode distance (*IED*)

Within a range of 0.5 cm to 1.5 cm, the efficiency of phosphorus removal was found to be increasing with an increase in inter-electrode distance. The maximum phosphorus removal was observed at an IED of 1.5 cm. At a low inter-electrode distance (1 cm), the movement of colloids and fluid through the electrode gap is obstructed resulting in accumulation of precipitates on the electrode surfaces. As a result, electrical resistance increases (Phalakornkule et al., 2009). Furthermore, colloidal particle interaction taking place at a low inter-electrode distance affects the flotation and settling of the precipitates which leads to increased resistance and affects total phosphorus removal (Shankar et al., 2014; Sridhar et al., 2011). Factorial plots for the inter-electrode distance are presented in Figure 7(d).

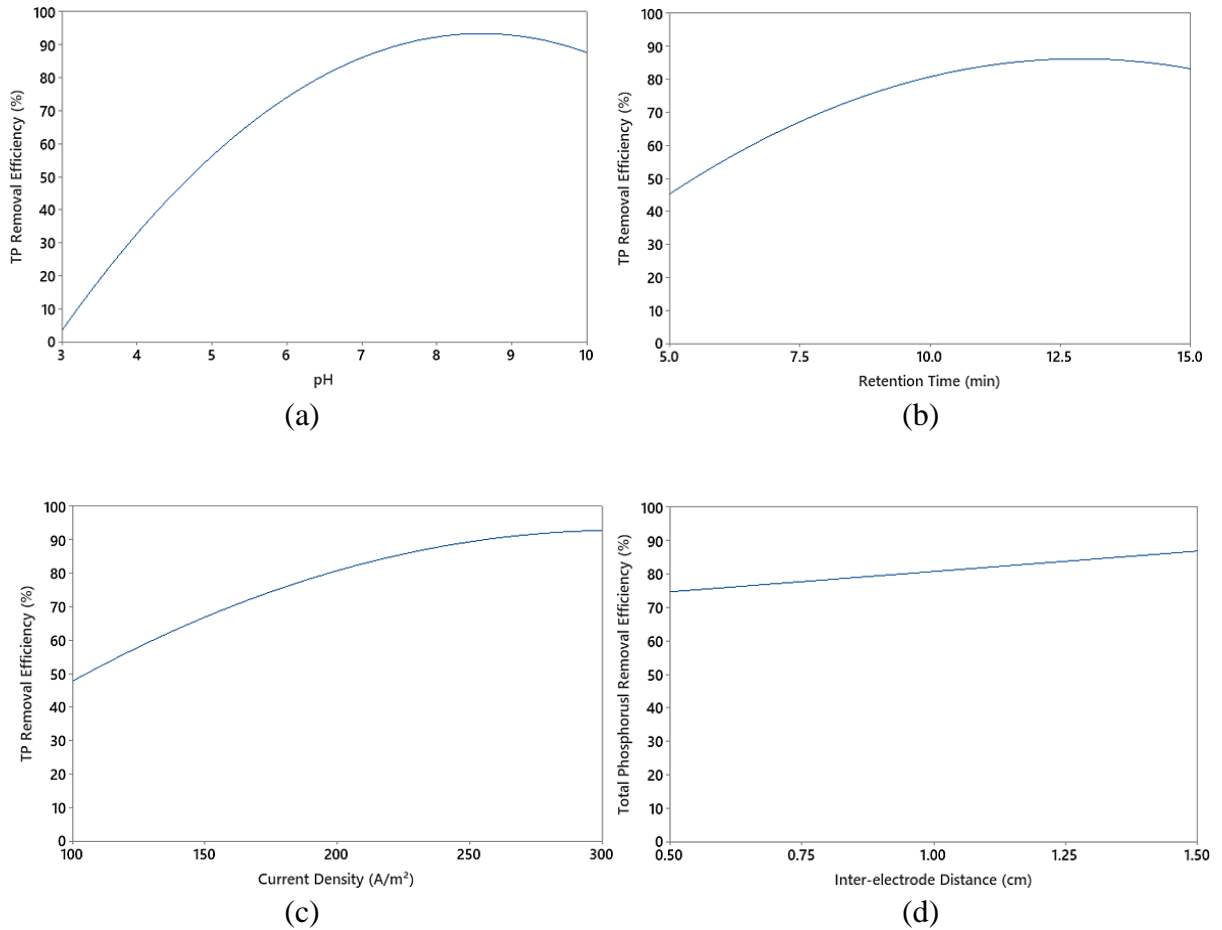


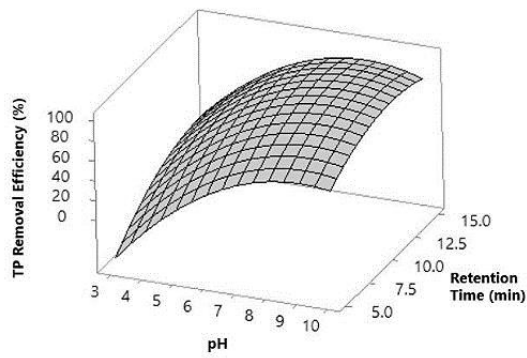
**Figure 7: Factorial plots for TP removal: Iron EC runs: (a) Initial pH (b) Retention Time (c) Current Density (d) Inter-electrode Distance**

#### 4.1.3 Variable Interaction and Response

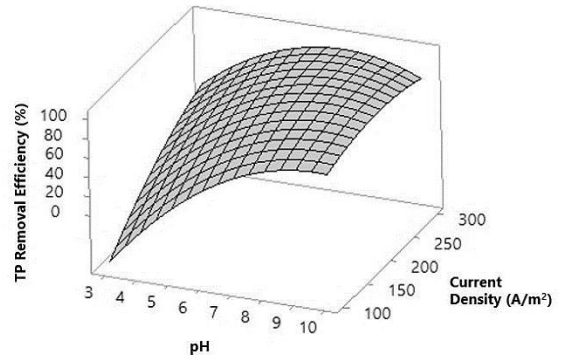
Response surface and contour plots were created changing the two factors and keeping another two factors constant (Center point). The significance of linear, squared and interaction terms is determined by comparing the corresponding p-values from the ANOVA results. For two-factor interactions, the relationship between the interaction

terms and the response is explained using response surfaces and contour plots. Figures 8 and 9 depict the plots of the response of the TP removal efficiency to the interaction terms. According to the interactive effect of pH and retention time, the efficiency of TP removal increased with increase in pH and retention time (RT), as shown in Figures 8(a) and 9(a). Figure 8(a) shows that when the pH is in the range of 6.5-10 and the retention time is greater than 8.5 mins, more than 90% removal efficiency can be achieved. Figures 8(b) and 9(b) depict the interaction plots for pH and current density. These plots show that TP removal efficiency increases with increasing pH and current density. Removals of more than 90% are shown in Figure 9(b) for pH ranges 6.5-10 and current densities greater than 175 A/m<sup>2</sup>. The interaction plots of pH and IED are depicted in Figures 8(c) and 9(c). It illustrates a higher removal efficiency at a pH range of 7.5-10 which is independent of IED. According to the interaction plot of retention time (RT) and inter-electrode distance (IED) described in Figures 8(d) and 9(d), TP removal increases with increase in retention time.

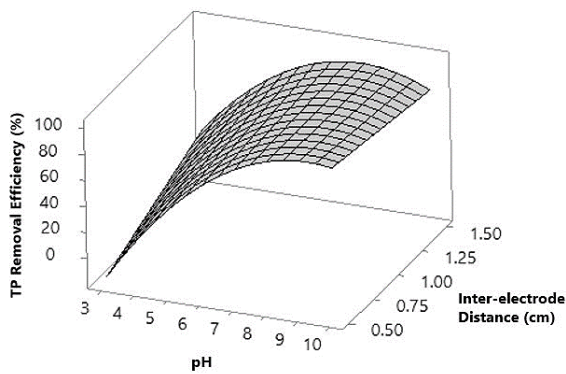
As shown in Figure 9(d), higher removal efficiency was observed at retention times greater than 11 min, and this was independent of IED. The interaction plots for current density (CD) and inter-electrode distance (IED) are depicted in Figures 8(e) and 9(e). Higher removal efficiency was observed when the CD was greater than 200 A/m<sup>2</sup> and the IED was greater than 0.87 cm.



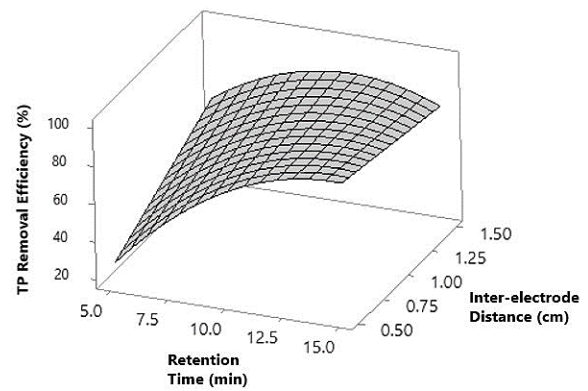
(a)



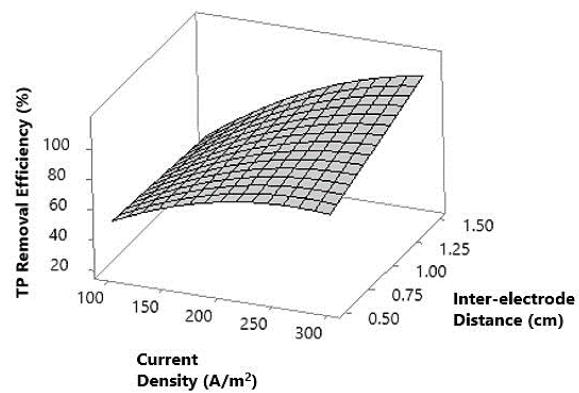
(b)



(c)



(d)



(e)

**Figure 8: Response surface plots for TP removal: Iron EC runs: (a) pH and retention time (b) pH and current density (c) pH and inter-electrode distance (d) retention time and inter-electrode distance (e) current density and inter-electrode distance**

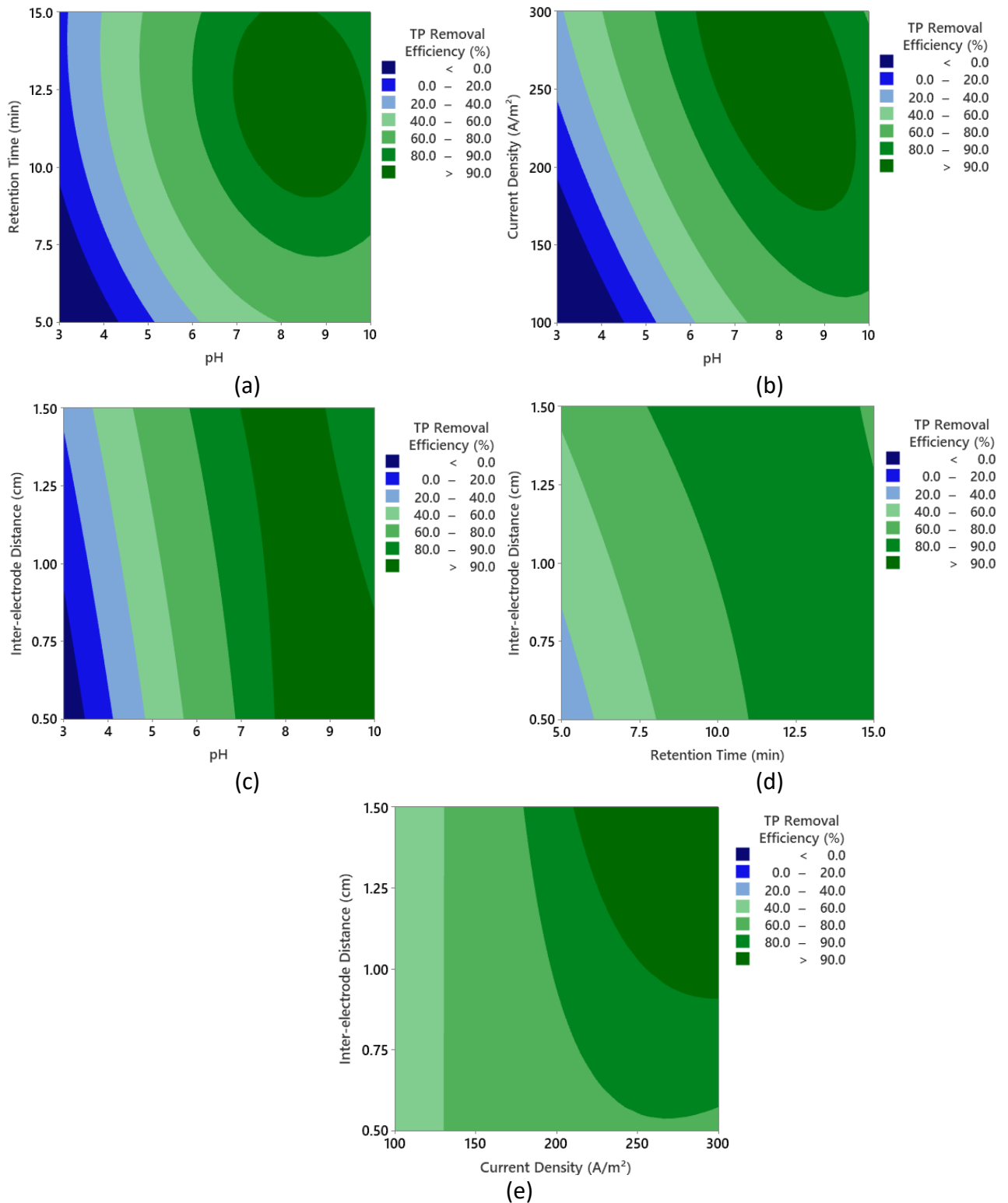


**Figure 9: Contour plots for TP removal: Iron EC runs: (a) pH and retention time (b) pH and current density (c) pH and inter-electrode distance (d) retention time and inter-electrode distance (e) current density and inter-electrode distance**

#### 4.1.4 Effect on COD Removal

Electrocoagulation method of water treatment is useful to target COD, turbidity, color, TSS and an array of contaminants. Selection of electrodes depends upon the composition of target compound that has to be removed from the wastewater. Electrocoagulation study carried out by Zaveri & Flora (2002) for the removal of phosphorus, nitrogen and COD from synthetic wastewater observed that removal efficiency of target contaminants was marginal. The primary reason suggested to be high solid concentration and COD content. For this study COD removal efficiency was considered to better understand the effect of electrocoagulation on COD removal when the target compound is phosphorus. The effect of the iron electrocoagulation process on COD removal was investigated using factorial plots generated with Minitab. Factorial plots describe the relationship between the process variables and response. Table 9 displays COD removal data for the iron electrocoagulation runs, and Figure 10 displays factorial plots.

The initial pH of the solution influences the stability of the metal hydroxide compounds formed during the reaction as well as the efficiency of COD removal. COD removal efficiency was found to increase with increasing pH from 3 to 10. The factorial plot for the initial pH shown in Figure 10(a) shows that high COD removal can be achieved for the iron electrode under alkaline conditions. Similar findings were observed by Bayramoglu et al. (2004). During this study, an increase in retention time resulted in an increase in COD removal efficiency. COD removal was found to increase with increasing current density, as illustrated in Figure 10(c). However, increasing the current density above 250 A/m<sup>2</sup> resulted in a decrease in COD removal efficiency. This could be because electrode

passivation occurs at high current densities, resulting in a decrease in metal ion addition. An increase in inter-electrode distance between 0.5 cm and 1.5 cm has no effect on COD removal efficiency. The factorial plot for inter-electrode distance is shown in Figure 10(d). However, when compared to 0.5 cm and 1.5 cm inter-electrode distances, 1 cm inter-electrode distance resulted in low COD removal.

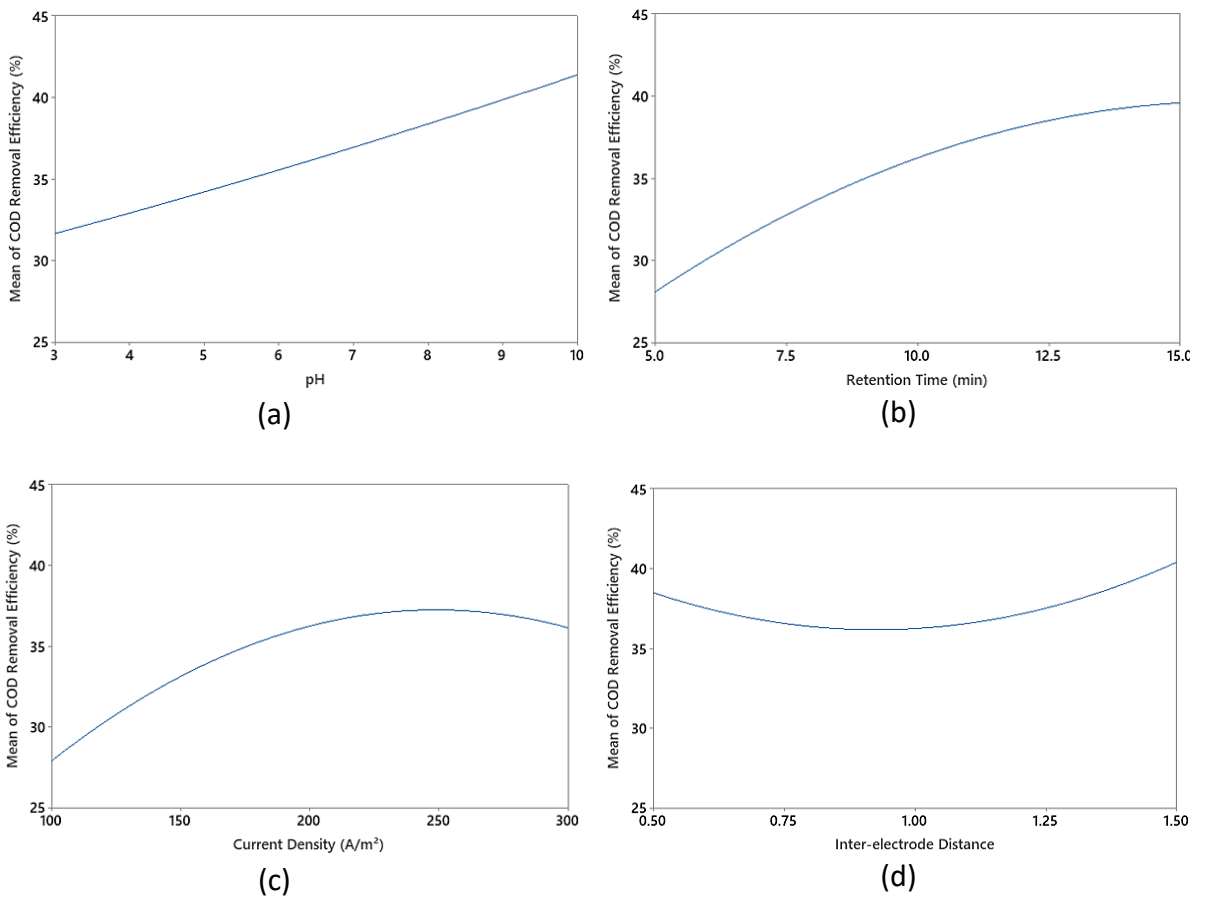


**Figure 10: Factorial plots for COD removal: Iron EC runs : (a) Initial pH (b) Retention Time (c) Current Density (d) Inter-electrode Distance**

**Table 9: COD removal data: Iron EC runs**

Run Order	Variables				Initial COD	Final COD	COD Removal Efficiency (%)
	pH	RT (mins)	CD (A/m <sup>2</sup> )	IED (cm)			
1	4.75	7.5	150	0.75	119.1 ± 5	85.60	28.13
2	8.25	7.5	150	0.75	119.1 ± 5	82.67	30.59
3	4.75	12.5	150	0.75	119.1 ± 5	81.60	31.49
4	8.25	12.5	150	0.75	119.1 ± 5	74.61	37.35
5	4.75	7.5	250	0.75	119.1 ± 5	80.26	32.61
6	8.25	7.5	250	0.75	119.1 ± 5	70.93	40.44
7	4.75	12.5	250	0.75	119.1 ± 5	77.60	34.84
8	8.25	12.5	250	0.75	119.1 ± 5	70.61	40.71
9	4.75	7.5	150	1.25	119.1 ± 5	87.94	26.16
10	8.25	7.5	150	1.25	119.1 ± 5	84.00	29.47
11	4.75	12.5	150	1.25	119.1 ± 5	74.93	44.92
12	8.25	12.5	150	1.25	119.1 ± 5	65.60	37.09
13	4.75	7.5	250	1.25	119.1 ± 5	81.28	31.76
14	8.25	7.5	250	1.25	119.1 ± 5	72.26	39.33
15	4.75	12.5	250	1.25	119.1 ± 5	77.60	34.84
16	8.25	12.5	250	1.25	119.1 ± 5	69.28	41.83
17	3	10	200	1	119.1 ± 5	82.61	30.64
18	10	10	200	1	119.1 ± 5	66.93	43.80
19	6.5	5	200	1	119.1 ± 5	85.27	28.40
20	6.5	15	200	1	119.1 ± 5	70.66	40.67
21	6.5	10	100	1	119.1 ± 5	85.60	28.13
22	6.5	10	300	1	119.1 ± 5	74.66	37.31
23	6.5	10	200	0.5	119.1 ± 5	71.95	39.59
24	6.5	10	200	1.5	119.1 ± 5	70.61	40.71
25	6.5	10	200	1	119.1 ± 5	73.28	38.47
26	6.5	10	200	1	119.1 ± 5	74.61	37.36
27	6.5	10	200	1	119.1 ± 5	77.28	35.11
28	6.5	10	200	1	119.1 ± 5	78.61	34.00
29	6.5	10	200	1	119.1 ± 5	79.92	32.90
30	6.5	10	200	1	119.1 ± 5	74.61	37.36
31	6.5	10	200	1	119.1 ± 5	73.28	38.47

\*Initial COD concentration includes the Mean ± SD of all the initial COD measurement

## 4.2 Magnesium Electrocoagulation System

Experimental runs were carried out as per central composite design (CCD), for modelling the TP removal. The independent process variables for the electrochemical struvite crystallization study are initial pH (pH), retention time (RT), current density (CD) and inter-electrode distance (IED). The levels for the independent process variables are shown in table 4. Table 10 lists the design matrix and run parameters as per central composite design for the phosphorus recovery by electrochemical struvite crystallization.

**Table 10: Design matrix: Magnesium EC runs**

Run Order	Coded Variables				TP Removal Efficiency (%)	
	pH	RT	CD	IED	Experimental	Predicted
1	-1	-1	-1	-1	84.69	84.86
2	1	-1	-1	-1	91.72	91.35
3	-1	1	-1	-1	92.47	91.94
4	1	1	-1	-1	94.99	95.44
5	-1	-1	1	-1	90.12	89.58
6	1	-1	1	-1	94.20	93.85
7	-1	1	1	-1	94.95	94.73
8	1	1	1	-1	95.92	96.01
9	-1	-1	-1	1	88.15	87.52
10	1	-1	-1	1	92.73	92.61
11	-1	1	-1	1	93.00	93.01
12	1	1	-1	1	95.12	95.11
13	-1	-1	1	1	92.83	92.24
14	1	-1	1	1	94.93	95.11
15	-1	1	1	1	95.77	95.79
16	1	1	1	1	95.99	95.68
17	-2	0	0	0	84.50	85.32
18	2	0	0	0	91.83	91.70

**Table 10: Design matrix: Magnesium EC runs (Continued)**

19	0	-2	0	0	88.88	90.00
20	0	2	0	0	97.40	97.65
21	0	0	-2	0	91.22	91.18
22	0	0	2	0	96.17	96.47
23	0	0	0	-2	93.60	93.90
24	0	0	0	2	95.85	96.23
25	0	0	0	0	94.49	93.82
26	0	0	0	0	93.45	93.82
27	0	0	0	0	94.30	93.82
28	0	0	0	0	93.82	93.82
29	0	0	0	0	92.85	93.82
30	0	0	0	0	94.12	93.82
31	0	0	0	0	93.96	93.82

#### 4.2.1 Statistical Analysis

Experimental runs were carried out according to the central composite design. Experimental run parameters are shown in Table 8. Experimental results were fitted to a quadratic equation using multiple regression analysis. The model summary is shown in Table 11. A high  $R^2$  value (>90%) indicated model's dependability. The results obtained from ANOVA analysis for the electrochemical struvite crystallization are shown in Table 12. Nonsignificant model terms ( $p < 0.05$ ) were eliminated for better fit of the model with the experimental data. The coefficient of determination was used to validate the model's fit to the experimental data. The coefficient of determination for this quadratic model was found to be 0.98 which is close to the adjusted  $R^2$  value and predicted  $R^2$  value. The normal probability plot depicts the normality of the experimental data. The normal probability plot of the residuals for the electrochemical struvite crystallization

(Figure 11) reveals that the majority of the points fall on a straight line. Furthermore, the high correlation between experimental and predicted data shown in Figure 12 indicates lower disparity.

**Table 11: Model summary: Magnesium EC runs**

Parameter	R <sup>2</sup> (%)	Adjusted R <sup>2</sup> (%)	Predicted R <sup>2</sup> (%)	P <sub>lof</sub>
Total Phosphorus	98.32	96.85	91.53	0.396

\*lof-lack of fit

**Table 12: ANOVA results: Magnesium EC runs**

Source	DF	Adj SS	Adj MS	F-Value	P-Value	Remarks
Model	14	278.264	19.8760	54.41	0.000	Significant
Linear	4	198.908	49.7270	136.11	0.000	Significant
A	1	61.039	61.0388	167.08	0.000	Significant
B	1	87.760	87.7602	240.22	0.000	Significant
C	1	41.987	41.9869	114.93	0.000	Significant
D	1	8.122	8.1222	22.23	0.000	Significant
Square	4	57.249	14.3122	39.18	0.000	Significant
A*A	1	50.759	50.7591	138.94	0.000	Significant
B*B	1	0.227	0.2271	0.62	0.442	Not significant
C*C	1	0.073	0.0726	0.20	0.662	Not Significant
D*D	1	2.707	2.7072	7.41	0.015	Significant
2-Way Interaction	6	22.107	3.6845	10.09	0.000	Significant
A*B	1	8.953	8.9526	24.51	0.000	Significant
A*C	1	4.908	4.9083	13.44	0.002	Significant
A*D	1	1.940	1.9398	5.31	0.035	Significant
B*C	1	3.736	3.7359	10.23	0.006	Significant
B*D	1	2.532	2.5316	6.93	0.018	Significant
C*D	1	0.039	0.0387	0.11	0.749	Not Significant
Error	16	5.845	0.3653			-
Lack-of-Fit	10	3.982	0.3982	1.28	0.396	Not significant
Pure Error	6	1.864	0.3106			-
Total	30	284.109				-

ANOVA results show that 11 out of the 14 model terms were found to be significant for electrochemical struvite crystallization. This includes linear terms such as pH (A), RT (B), CD (C) and IED (D), as well as squared terms such as  $pH^2$  ( $A^2$ ), and interaction terms such as  $pH \cdot RT$  (AB),  $pH \cdot CD$  (AC),  $pH \cdot IED$  (AD),  $RT \cdot CD$  (BC)  $RT \cdot IED$  (BD), The quadratic model for TP removal efficiency was expressed as equation (16).

*Total Phosphorus Removal Efficiency*(%)

$$\begin{aligned}
 &= 93.821 + 1.595pH + 1.912RT + 1.323CD + 0.582IED \\
 &- 1.329pH \cdot pH + 0.311IED \cdot IED - 0.748pH \cdot RT \\
 &- 0.554pH \cdot CD - 0.348pH \cdot IED - 0.483RT \cdot CD \\
 &- 0.398RT \cdot IED
 \end{aligned} \tag{16}$$

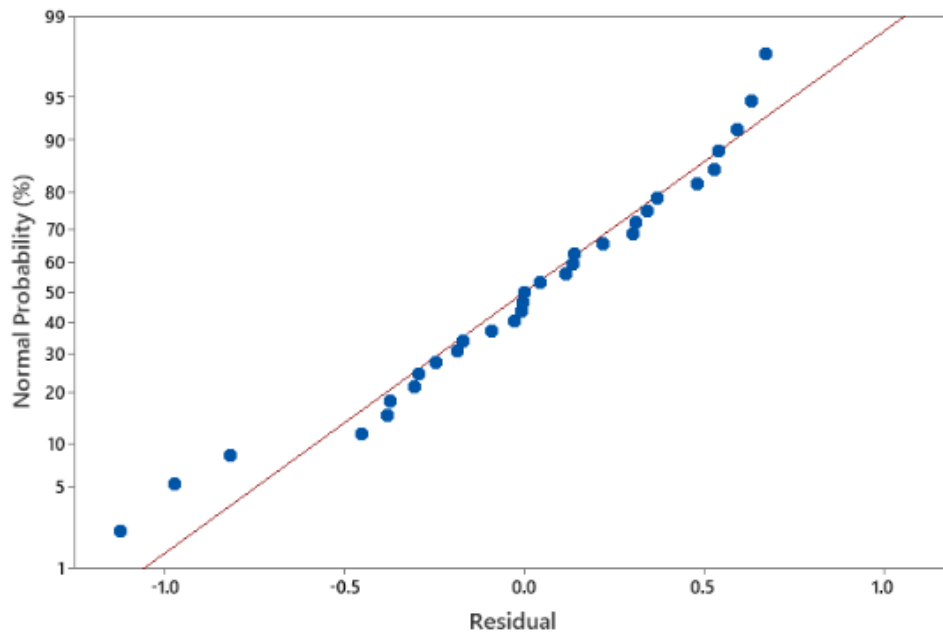


**Figure 11: Normal probability plot of the residuals**

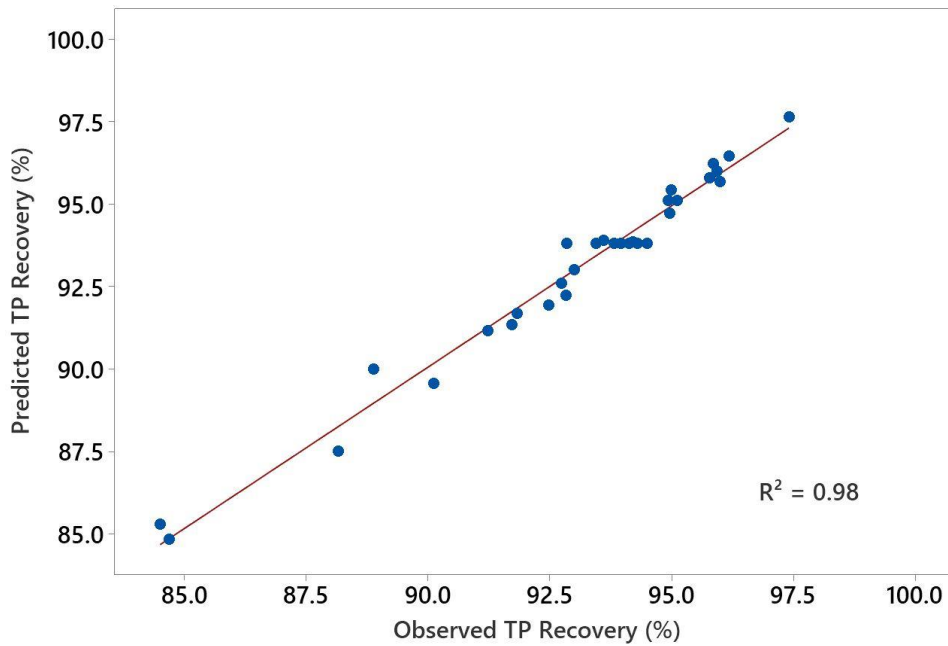


**Figure 12: Predicted vs Observed TP recovery efficiency**

For phosphorus recovery by electrochemical struvite crystallization using a magnesium electrocoagulation reactor, retention time was found to be the most significant factor among linear terms, while initial pH was found significant among squared terms. Among interaction terms influencing the response, the interaction of initial pH and retention time was observed to be significant. In case of iron electrodes, initial pH is the most significant factor among linear and quadratic terms. This is due to the fact that magnesium electrodes have a much slower phosphorus removal rate than iron electrodes, necessitating a longer retention time to recover phosphorus from phosphorus-rich effluent. This could be because of the fact that phosphorus removal using magnesium electrodes was independent of metal dosing and was dependent on the solubility of magnesium ions (Devlin et al., 2019). A longer retention time for

magnesium electrodes results in more hydroxide ions being added to the solution, which raises the pH and thus solubility. Struvite crystallization from anaerobic effluent is favoured in alkaline condition because of low solubility of struvite. It is the primary reason that the pH range for the magnesium electrocoagulation system varies from 6.5 to 10 whereas for the iron electrocoagulation system it varies from pH 3 to 10.

#### 4.2.2 Effect of Independent Process Variables

##### 4.2.2.1 Initial pH (*pH*)

Initial pH is a critical factor for phosphorus recovery in the form of struvite. It affects the conductivity of the wastewater as well as the dissolution of electrode material. Factorial plot for initial pH is shown in Figure 13(a). For this study, total phosphorus recovery was found to be moderate at slightly acidic pH (6.5) and found to be increasing with an increase in pH to 9. Further increase in pH causes a reduction in TP recovery efficiency. An increase in pH beyond the optimum value (pH=9) causes a decrease in ammoniacal nitrogen concentration in the wastewater due to the formation of ammonia gas, thereby affecting the ratio of nitrogen and phosphorus (Stumm & Morgan, 1996). pH affects the solubility of the struvite. According to Ohlinger et al. (1998), the solubility of struvite was found to be decreasing with an increase in pH within the range of 6 to 8. However, the pH of low solubility was observed at a pH value of 9 by Buchannan et al. (1994). Higher struvite solubility and electrode passivation can explain the decrease in TP recovery above pH 9.

#### 4.2.2.2 Retention Time (*RT*)

TP recovery using electrochemical struvite precipitation was found to be increasing with an increase in retention time. Similar findings were made with iron electrodes. However, magnesium electrodes require a longer retention time compared to iron electrodes in order to achieve similar removal efficiency. The factorial plot of retention time vs TP recovery is shown in Figure 13(b). This is because of the fact that extent of metal ions addition from the anode into the solution for a constant current density is dependent on the retention time.

#### 4.2.2.3 Current Density (*CD*)

The current density affects the rate of production of metal ions (coagulant), according to Faraday's law, resulting in higher phosphorus recovery. Furthermore, an increase in current density causes increase in the rate of bubble formation while decreasing the size of the bubbles. Both effects are advantageous for high pollutant removal via H<sub>2</sub> flotation (Holt et al., 2002; Kobya et al., 2006). While current density has an effect on metal ion dosing, it has no effect on the concentration of metal ions in the solution when electrode materials of same valency are used. Factorial plot for current density is shown in Figure 13(c). Within a current density range of 100 A/m<sup>2</sup> to 300A/m<sup>2</sup>, phosphorus recovery efficiency is found to increase with increasing current density.

#### 4.2.2.3 Inter-electrode Distance (*IED*)

The inter-electrode distance has a negligible impact on the performance of an electrocoagulation system as shown in Figure 13(d). Increase in inter-electrode distance

causes an increase in IR drop (potential drop), resulting in increased energy consumption. Although the change is minor, increase in inter-electrode distance from 0.5 cm to 0.75 cm has a negative impact on TP removal. However, increasing the inter-electrode distance from 0.75cm to 1.5 cm increases TP recovery, though the efficiency gain is slight. The maximum phosphorus removal was observed at an IED of 1.5 cm within the range of 0.5 cm to 1.5 cm. For the iron electrocoagulation system, similar observations were made where TP removal was found to be increasing with an increase in inter-electrode distance within the range of 0.5 cm to 1.5 cm. This is because colloidal

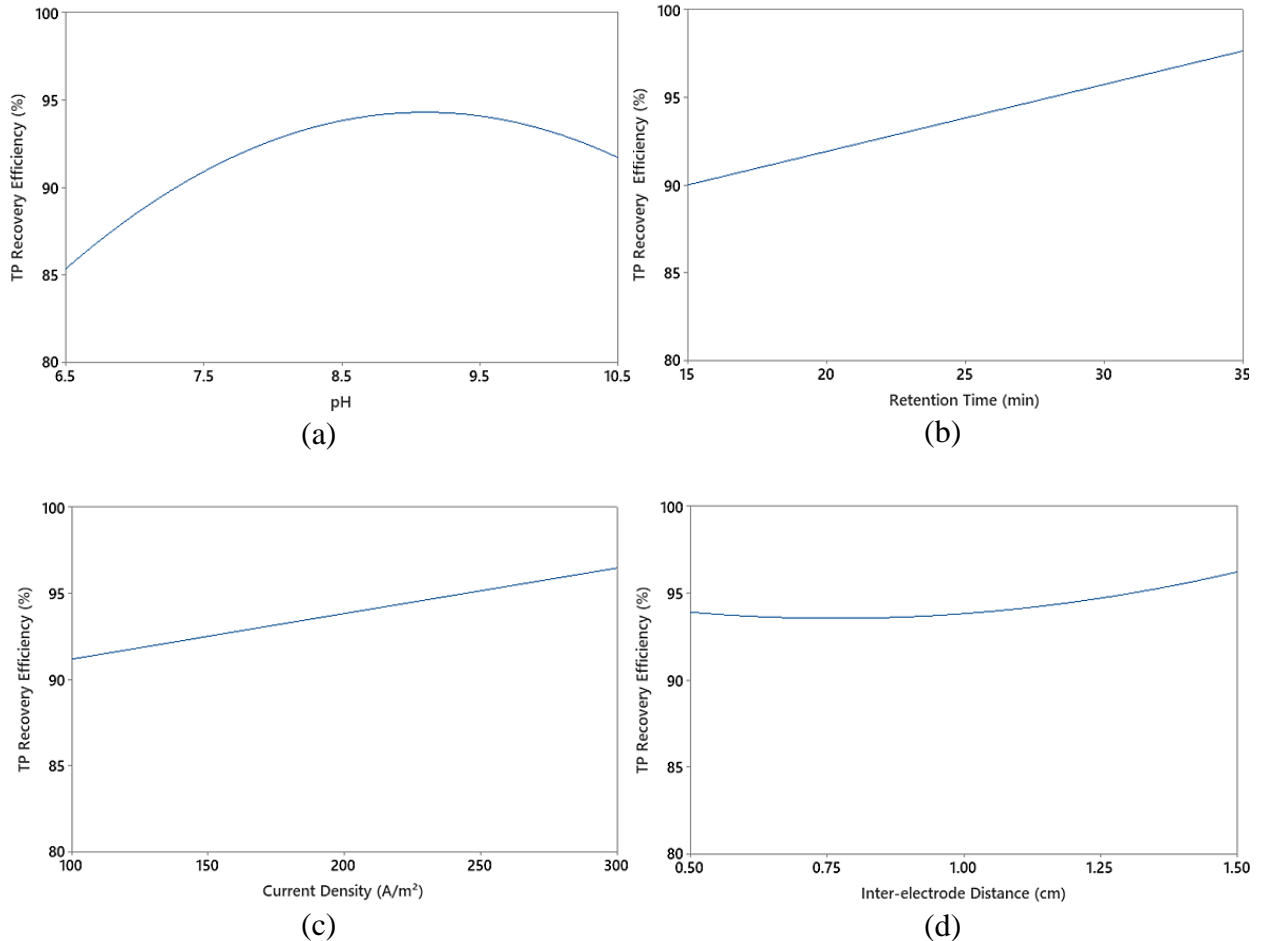


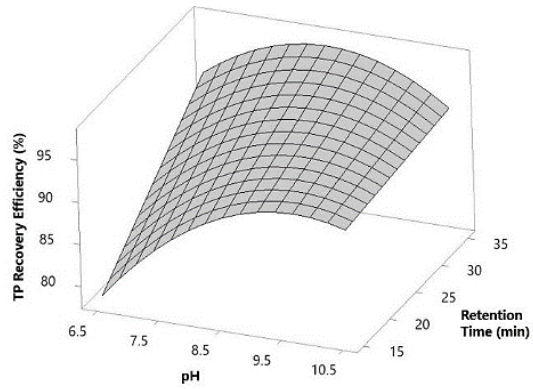
**Figure 13: Factorial plots for TP recovery: Magnesium EC runs: (a) Initial pH (b) Retention Time (c) Current Density (d) Inter-electrode Distance**

particle interaction affects the settling and flotation characteristics of the precipitates at a low inter-electrode distance (1 cm), resulting in high electrical resistance and less removal (Shankar et al., 2014; Sridhar et al., 2011).

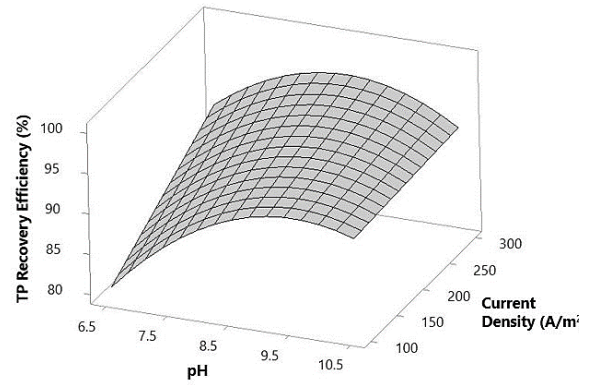
#### 4.2.3 Variable Interaction and Response

Response surface and contour plots are used to demonstrate the interaction between the independent process variables and their impact on the response variable. This study considers two-factor interactions. Figures 13 and 14 show response surface and contour plots for significant interaction terms ( $p < 0.05$ ). Figures 14(a) and 15(a) show the interaction plot of pH and retention time. Total phosphorus recovery using electrochemical struvite crystallization increases with increasing pH and retention time, as shown in this plot. However, at very high pH, the efficiency of TP recovery is found to be decreasing. The maximum phosphorus recovery was observed at the pH of 9. The optimal point for retention time was found at the maximum value considered for the retention time ( $t = 35$  mins). Surface plot and contour plot corresponding to initial pH and current density is shown in figures 14(b) and 15(b). TP recovery was found to be increasing with increasing pH until it reached 9 and with increasing current density. The pH range of 8.5 to 9.5 and higher current density were found to be optimal for the recovery. Figures 14(c) and 15(c) show an upward trend for both parameters in the interaction plot for current density and retention time, indicating that increasing both parameters have a positive effect on TP recovery. The interaction plot of retention time and inter-electrode distance shown in Figures 14(d) and 15(d) indicate that TP recovery

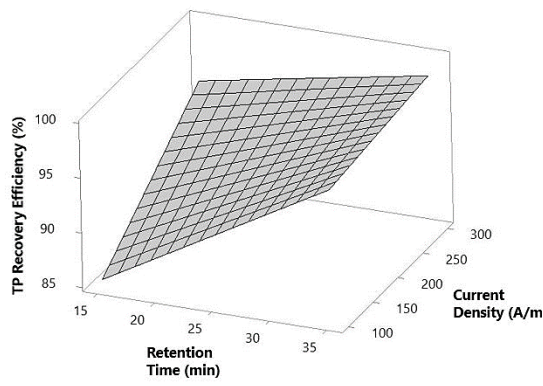
of more than 95% can be expected at a retention time of more than 27.5 minutes and is independent of inter-electrode distance (pH=8.5, CD=200A/m<sup>2</sup>). Figures 14(e) and 15(e) depict the interaction plot for pH and inter-electrode distance, which shows that maximum phosphorus recovery can be achieved at a pH of 9 and an inter-electrode distance greater than 1.25 cm.



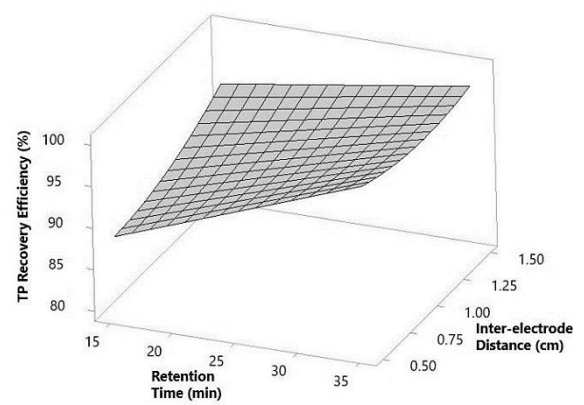
(a)



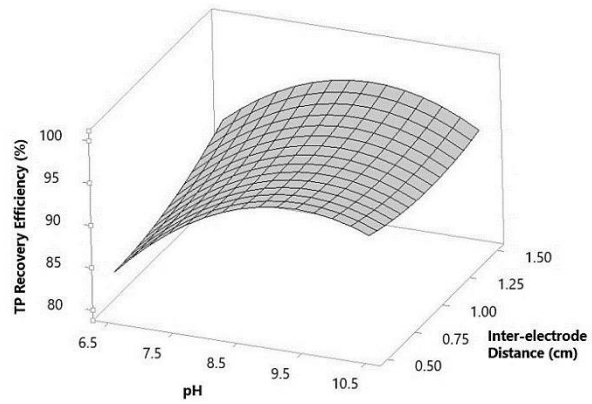
(b)



(c)



(d)



(e)

**Figure 14: Response surface plots for TP recovery: Magnesium EC runs: (a) pH and retention time (b) pH and current density (c) retention time and current density (d) retention time and inter-electrode distance (e) pH and inter-electrode distance**

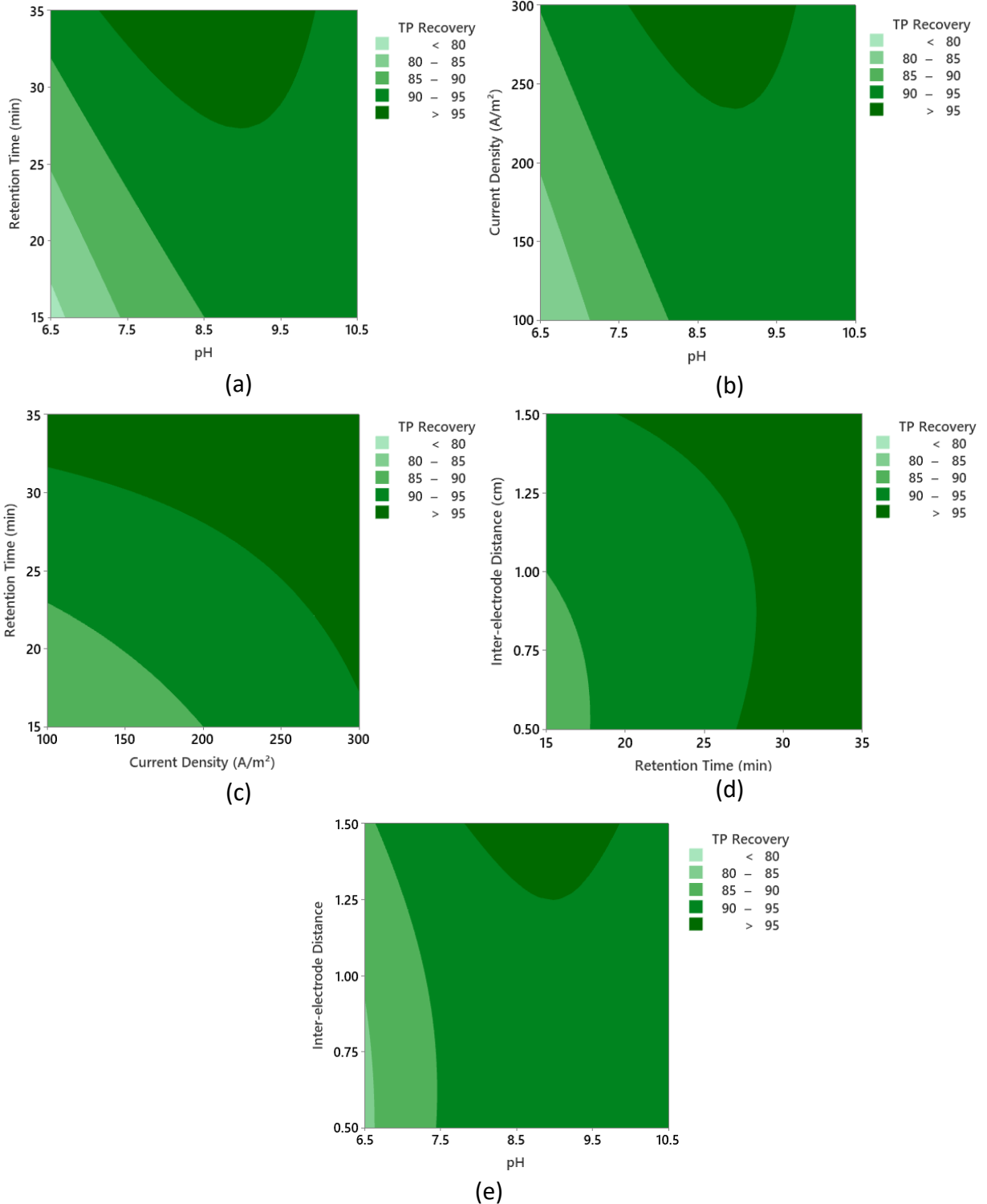


**Figure 15: Contour plots for TP recovery: Magnesium EC runs: (a) pH and retention time (b) pH and current density (c) current density and retention time (d) retention time and inter-electrode distance (e) pH and inter-electrode distance**

#### 4.2.4 Effect on COD Removal

The effect of the magnesium electrocoagulation system on COD removal is investigated using factorial plots generated with Minitab. Factorial plots illustrate the relationship between the process variables and response. Table 13 displays COD removal data for the magnesium electrode, and Figure 16 displays factorial plots.

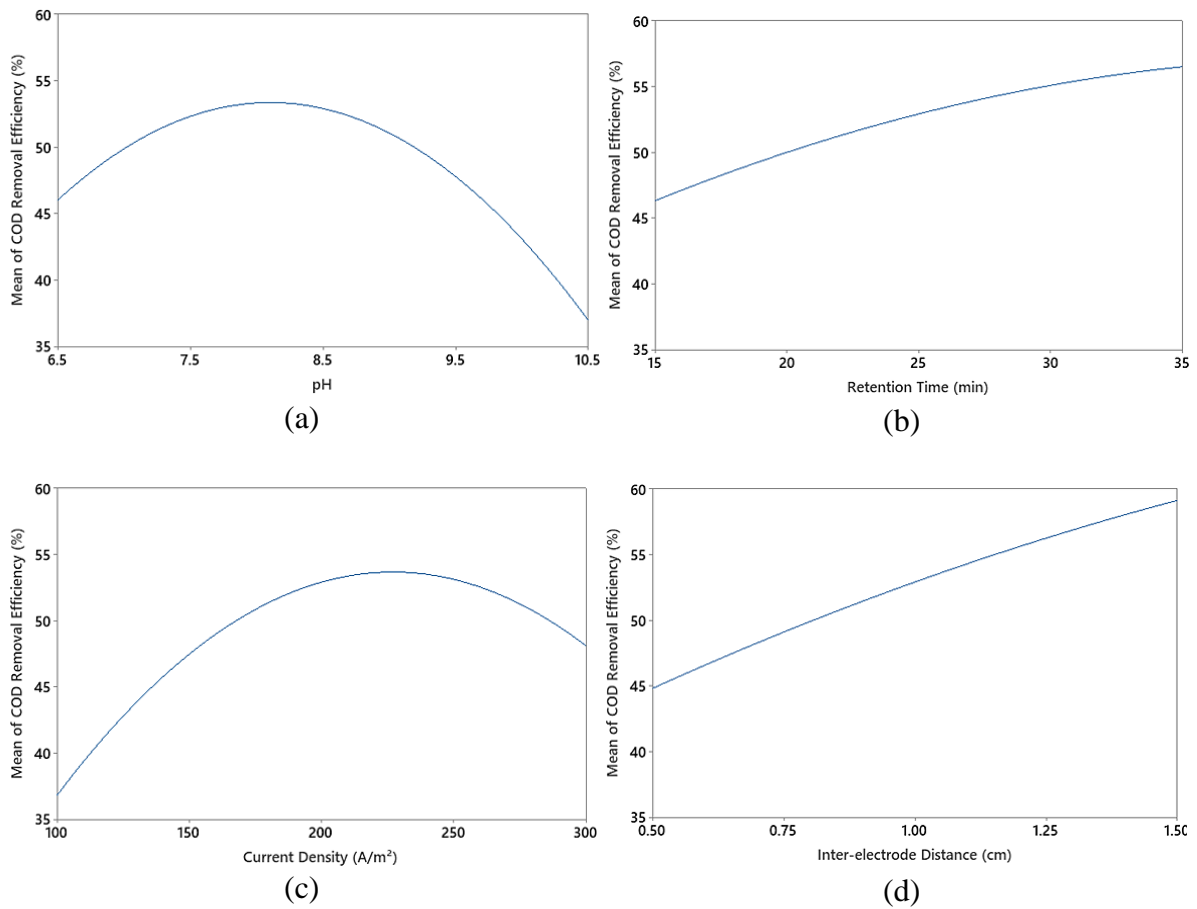


**Figure 16: Factorial plots for COD removal: Magnesium EC runs: (a) Initial pH (b) Retention Time (c) Current Density (d) Inter-electrode Distance**

**Table 13: COD removal data: Magnesium EC runs**

Run Order	Variables				Initial COD	Final COD	COD Removal Efficiency (%)
	pH	RT (mins)	CD (A/m <sup>2</sup> )	IED (cm)			
1	7.5	20	150	0.75	119.1 ± 5	78.69	33.93
2	9.5	20	150	0.75	119.1 ± 5	86.69	27.21
3	7.5	30	150	0.75	119.1 ± 5	57.36	51.84
4	9.5	30	150	0.75	119.1 ± 5	84.03	29.45
5	7.5	20	250	0.75	119.1 ± 5	64.03	46.24
6	9.5	20	250	0.75	119.1 ± 5	72.03	39.52
7	7.5	30	250	0.75	119.1 ± 5	62.67	47.38
8	9.5	30	250	0.75	119.1 ± 5	65.33	45.15
9	7.5	20	150	1.25	119.1 ± 5	66.66	44.03
10	9.5	20	150	1.25	119.1 ± 5	58.67	50.74
11	7.5	30	150	1.25	119.1 ± 5	57.33	51.86
12	9.5	30	150	1.25	119.1 ± 5	50.67	57.46
13	7.5	20	250	1.25	119.1 ± 5	45.33	61.94
14	9.5	20	250	1.25	119.1 ± 5	53.33	55.22
15	7.5	30	250	1.25	119.1 ± 5	53.6	55.00
16	9.5	30	250	1.25	119.1 ± 5	80.27	32.60
17	6.5	25	200	1.00	119.1 ± 5	66.93	43.80
18	10.5	25	200	1.00	119.1 ± 5	66.6	44.08
19	8.5	15	200	1.00	119.1 ± 5	69.6	41.56
20	8.5	35	200	1.00	119.1 ± 5	40.27	66.19
21	8.5	25	100	1.00	119.1 ± 5	74.93	37.09
22	8.5	25	300	1.00	119.1 ± 5	56.27	52.75
23	8.5	25	200	0.50	119.1 ± 5	53.6	55.00
24	8.5	25	200	1.50	119.1 ± 5	54.93	53.88
25	8.5	25	200	1.00	119.1 ± 5	60.27	49.40
26	8.5	25	200	1.00	119.1 ± 5	56.27	52.75
27	8.5	25	200	1.00	119.1 ± 5	54.93	53.88
28	8.5	25	200	1.00	119.1 ± 5	52.27	56.11
29	8.5	25	200	1.00	119.1 ± 5	57.6	51.64
30	8.5	25	200	1.00	119.1 ± 5	56.27	52.75
31	8.5	25	200	1.00	119.1 ± 5	54.93	53.88

\*Initial COD concentration includes the Mean ± SD of all the initial COD measurement

Electrochemical struvite precipitation destroys organics during the process. During the process, COD removal was found to increase with increasing in pH until 8. Further increase in pH has a negative impact on COD removal. COD removal was found to be increasing with an increase in retention time and inter-electrode distance. COD removal was also found to be increasing with an increase in current density until it reached 225 A/m<sup>2</sup>. Further increase in current density causes a decrease in COD removal efficiency during the process. However, the initial COD concentration for the anaerobic effluent used for this study was low.

#### 4.2.5 Effect on Ammonia-Nitrogen Removal

Struvite crystals are composed of magnesium, phosphate, and ammonia. Both phosphorus and ammonia are recovered from wastewater in this process. It is necessary to study the ammonia concentration in the treated effluent to understand the recovery ratio of these two parameters. The results for NH<sub>3</sub>-N removal during electrochemical struvite precipitation are shown in Table 14. This demonstrates that ammonia removal from anaerobic bioreactor effluent is minimal when compared to total phosphorus. The maximum amount of ammonia removal observed during this study was 31.25 ± 1.51%, while total phosphorus was observed to be 94.12 ± 0.78% for the electrocoagulation run with initial pH of 8.5, retention time of 25 mins, current density of 200 A/m<sup>2</sup>, and inter-electrode distance of 1 cm. Similar observations were observed by Le Corre et al. (2009). This can be explained by the fact that the concentration of NH<sub>3</sub>-N used for this study is more than three times that of total phosphorus, whereas the ideal ratio should be 1:1. This may be one of the causes of the high residual NH<sub>3</sub>-N concentration in the treated

effluent. From the factorial plots of process variables shown in Figure 17, the removal of  $\text{NH}_3\text{-N}$  was found to increase with increasing pH, retention time, current density and inter-electrode distance until it reached the center point value (pH=8.5, RT=25 mins, CD=200  $\text{A}/\text{m}^2$ , IED=1 cm). Further increase in value of process variables has a negative effect on  $\text{NH}_3\text{-N}$  removal during electrochemical struvite precipitation.

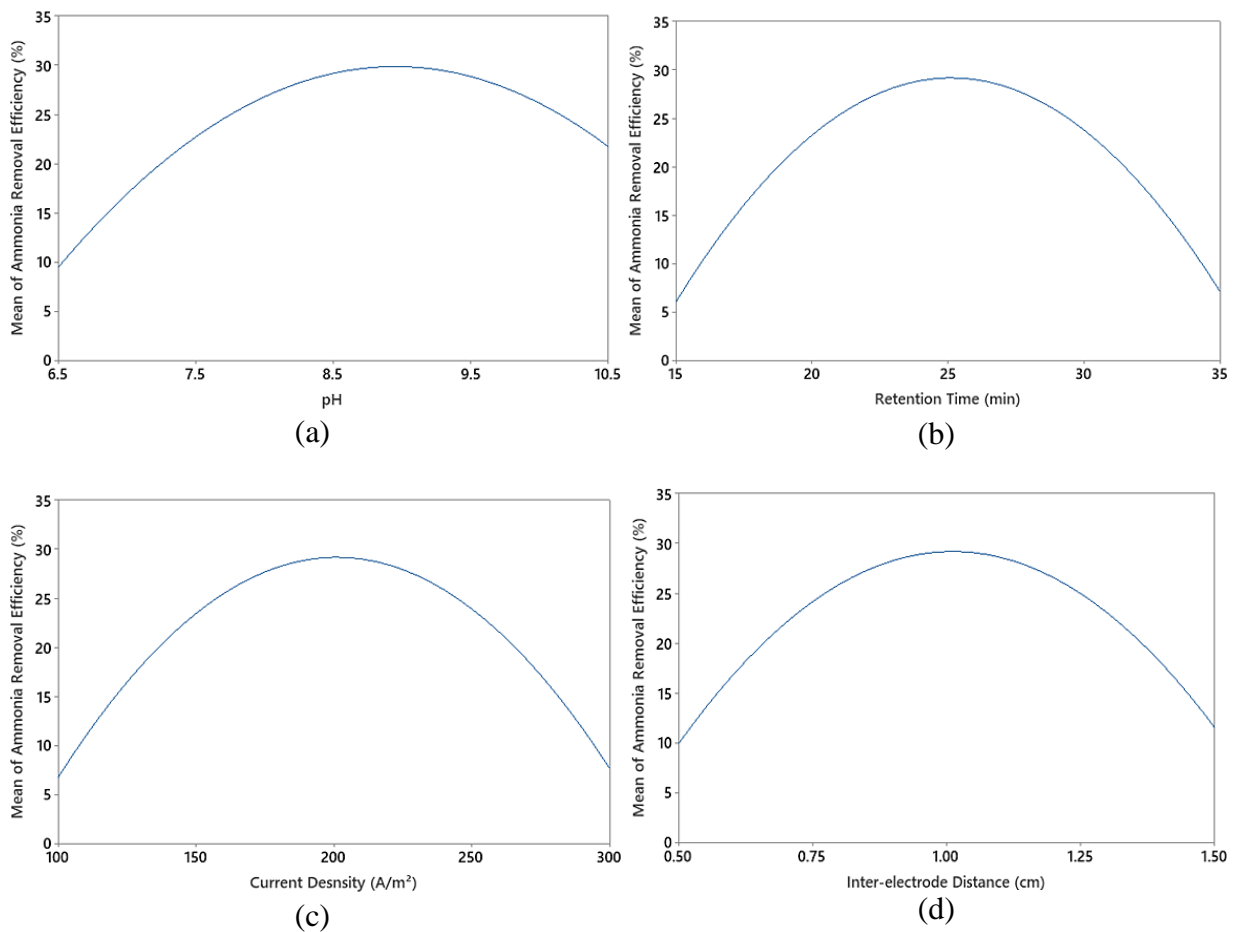


**Figure 17: Factorial plots for  $\text{NH}_3\text{-N}$  removal: Magnesium EC runs: (a) Initial pH (b) Retention Time (c) Current Density (d) Inter-electrode Distance**

**Table 14: NH<sub>3</sub>-N removal data: Magnesium EC runs**

Run Order	Variables				Initial NH <sub>3</sub> -N Concentration (mg/L)	Final NH <sub>3</sub> -N Concentration (mg/L)	NH <sub>3</sub> -N Removal Efficiency (%)
	pH	RT (mins)	CD (A/m <sup>2</sup> )	IED (cm)			
1	7.5	20	150	0.75	160 ± 2.5	156	2.50
2	9.5	20	150	0.75	160 ± 2.5	141.6	11.50
3	7.5	30	150	0.75	160 ± 2.5	140.4	12.25
4	9.5	30	150	0.75	160 ± 2.5	141.6	11.50
5	7.5	20	250	0.75	160 ± 2.5	141.2	11.75
6	9.5	20	250	0.75	160 ± 2.5	141.2	11.75
7	7.5	30	250	0.75	160 ± 2.5	146.8	8.25
8	9.5	30	250	0.75	160 ± 2.5	143.4	10.37
9	7.5	20	150	1.25	160 ± 2.5	143.2	10.50
10	9.5	20	150	1.25	160 ± 2.5	137.8	13.87
11	7.5	30	150	1.25	160 ± 2.5	147.4	7.87
12	9.5	30	150	1.25	160 ± 2.5	142.6	10.88
13	7.5	20	250	1.25	160 ± 2.5	141.6	11.50
14	9.5	20	250	1.25	160 ± 2.5	138.8	13.25
15	7.5	30	250	1.25	160 ± 2.5	155.2	3.00
16	9.5	30	250	1.25	160 ± 2.5	142.8	10.75
17	6.5	25	200	1.00	160 ± 2.5	154.4	3.50
18	10.5	25	200	1.00	160 ± 2.5	116.4	27.25
19	8.5	15	200	1.00	160 ± 2.5	157.2	1.75
20	8.5	35	200	1.00	160 ± 2.5	142.4	11.00
21	8.5	25	100	1.00	160 ± 2.5	151.2	5.50
22	8.5	25	300	1.00	160 ± 2.5	146.4	8.50
23	8.5	25	200	0.50	160 ± 2.5	146.4	8.50
24	8.5	25	200	1.50	160 ± 2.5	140	12.50
25	8.5	25	200	1.00	160 ± 2.5	116	27.50
26	8.5	25	200	1.00	160 ± 2.5	110.8	30.75
27	8.5	25	200	1.00	160 ± 2.5	115.2	28.00
28	8.5	25	200	1.00	160 ± 2.5	115.6	27.75
29	8.5	25	200	1.00	160 ± 2.5	112	30.00
30	8.5	25	200	1.00	160 ± 2.5	110	31.25
31	8.5	25	200	1.00	160 ± 2.5	113.6	29.00

\*Initial NH<sub>3</sub>-N concentration includes the Mean ± SD of all the initial NH<sub>3</sub>-N measurement

### 4.3 Optimization

The economic sustainability of a process can be evaluated by investigating the feasibility of the treatment method, optimization of independent variables and design of the reactor.

#### 4.3.1 Optimization for Fe-Electrocoagulation System

Optimized conditions for the TP removal efficiency were obtained after evaluating the significance of independent process variables. The factors affecting TP removal were optimized using MiniTab software (version 20). This study found that optimal conditions are a pH of 6.75, a retention time of 11.06 minutes, a current density of 300 A/m<sup>2</sup>, and an inter-electrode distance of 1.5 cm. At the optimum conditions, the model predicts that all the phosphorus present in the anaerobic bioreactor effluent will be removed. Confirmation runs were performed using the model's predicted optimal conditions. Table 15 displays the experimental results under optimal conditions.

**Table 15: Verification of experimental results: Iron EC runs**  
(pH = 6.75, RT = 11.06 min, CD = 300A/m<sup>2</sup>, IED = 1.5 cm, V = 11.57 V)

<b>Optimum Conditions</b>	<b>TP removal efficiency (%)</b>
Model response	100
Experimental results	98.05
Error	1.95
Standard deviation	± 0.75

Electrocoagulation sludge of 276 ± 11 mg was obtained from a litre of anaerobic effluent during the optimal electrocoagulation runs. XRD analysis of the sludge was carried out to find out the presence of crystalline compounds. The results as shown in

Figure 18 shows the amorphous nature of the sludge. EDS analysis of the sludge revealed the presence of C, O, P, Cl, Ca, and Fe as primary elements. The presence of phosphorus indicates that it has been successfully adsorbed onto iron hydroxides. The formation of amorphous structures with large grooves (binding sites) was revealed by SEM image (Figure 19) of the sludge.

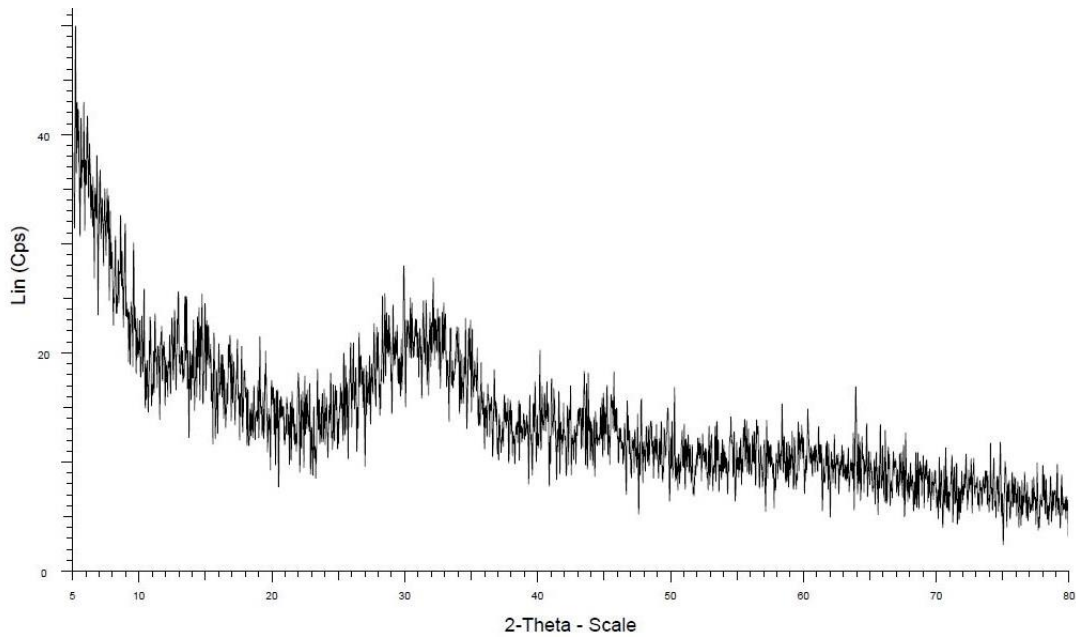


**Figure 18: XRD spectra of the iron EC sludge**

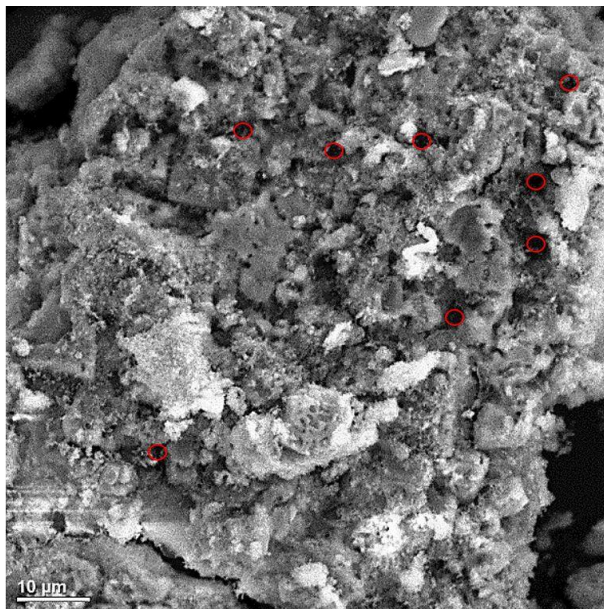


**Figure 19: SEM image of the iron EC sludge**

TP removal under experimental conditions was found to be 98.05%, which agrees with the predicted response. At optimal conditions, the energy consumption was determined to be 1.28 kWh/m<sup>3</sup>.

#### 4.3.2 Optimization for Mg-Electrocoagulation System

Optimized parameters for electrochemical struvite precipitation were obtained from the response optimization study using MiniTab software (version 20). A pH of 8.4, a retention time of 35 minutes, a current density of 300 A/m<sup>2</sup>, and an inter-electrode distance of 0.5 cm were found to be optimal for maximizing phosphorus recovery. The statistical model predicts that under optimal conditions, all of the phosphorus in the anaerobic bioreactor effluent will be recovered. Confirmatory runs were carried out under optimal operating conditions. Table 16 displays the experimental results under optimal conditions. XRD analysis of the precipitate obtained from this study shown in Figure 20 confirmed the presence of struvite as the only crystalline compound.

**Table 16: Verification of experimental results: Magnesium EC runs**  
(pH = 8.4, RT = 35 min, CD = 300A/m<sup>2</sup>, IED = 0.5 cm, V = 6.7 V)

<b>Optimum Conditions</b>	<b>TP removal efficiency (%)</b>
Model response	100
Experimental results	97.30
Error	3.02
Standard deviation	± 0.55

TP recovery during this study was found to be 97.30% which agrees with the predicted response. Energy consumption during optimal operating conditions was found to be 2.35 kWh/m<sup>3</sup>. When compared to previous studies, this study revealed phosphorus

recovery in a very short retention time for magnesium electrodes. The energy consumption for this study was found to be higher when compared to the iron electrocoagulation system (manuscript under review) in order to achieve comparable recovery efficiency. However, the precipitate obtained from this study can be used directly in agriculture, whereas the precipitate obtained from the iron electrocoagulation system requires additional processing for extraction, increasing the recovery cost.

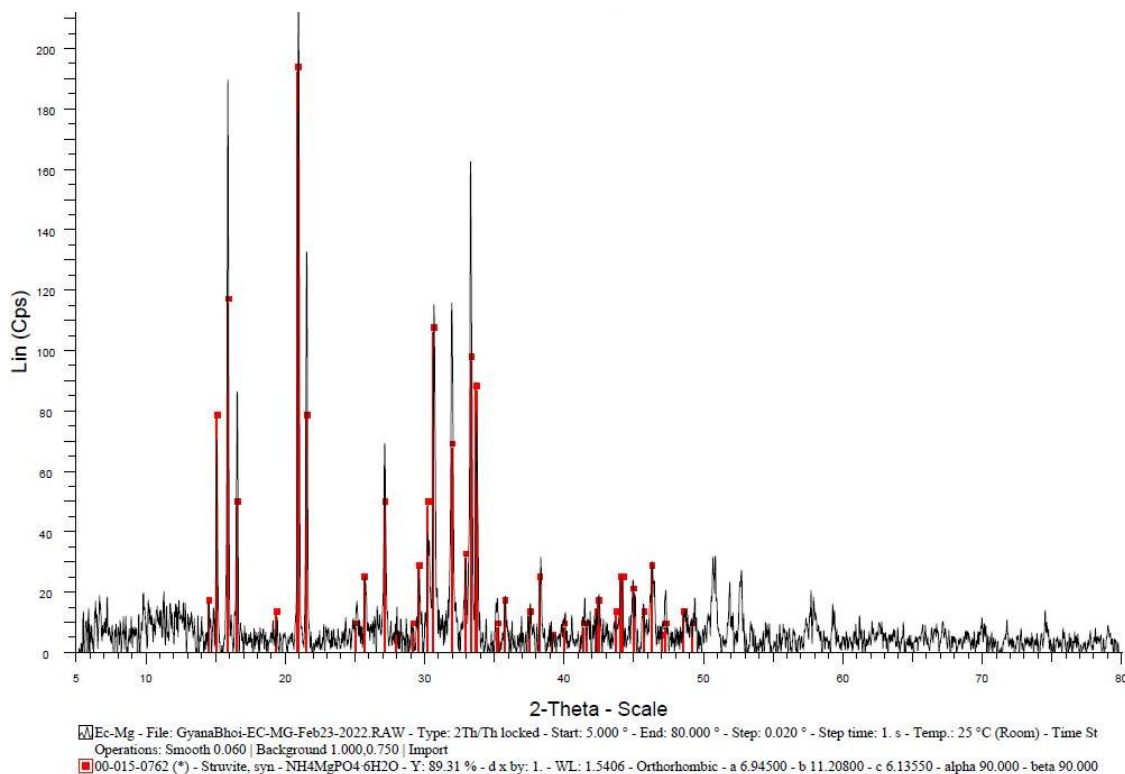


**Figure 20: XRD spectra of the magnesium EC sludge**

XRD analysis of the precipitate obtained from the magnesium electrocoagulation reactor showed the presence of struvite as the only crystalline compound. When compared to the commercially available struvite (crystal Green, Ostara) studied by Kékedy-Nagy et al.( 2020), the XRD pattern obtained from this study showed a high degree of similarity in terms of peak position and intensity. The results of SEM analysis

of the precipitate are shown in Figure 21. The crystals were a mix of orthorhombic and spherical shapes. Some clusters were also observed without any distinct shape.

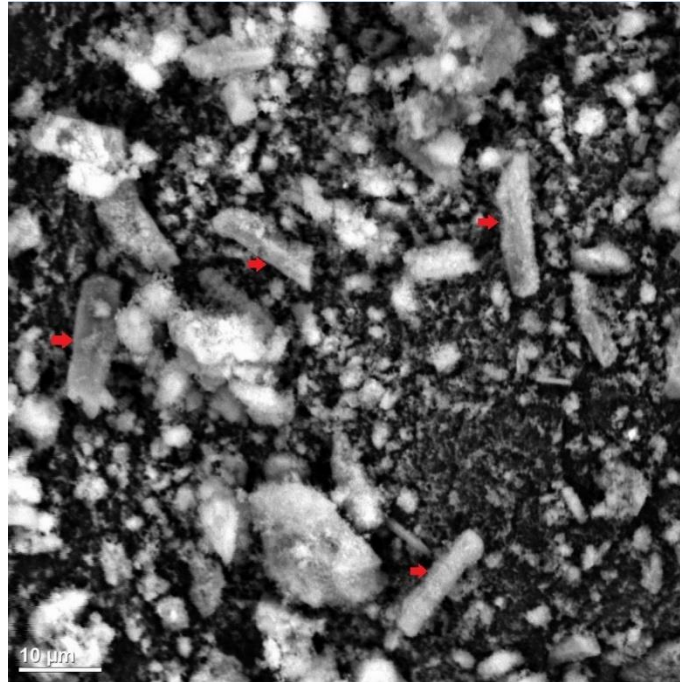


**Figure 21: Electron micrograph of struvite crystals**

#### 4.4 Kinetics of TP Removal

##### 4.4.1 Iron Electrocoagulation System

The kinetics of phosphorus removal were studied, with the experimental runs carried out under optimal conditions (pH = 6.75, retention time = 11.06 min, current density = 300A/m<sup>2</sup>, inter-electrode distance = 1.5 cm). The rate of phosphorus removal from the anaerobic effluent equation has been expressed using the given first-order rate law (17).

$$-V \left( \frac{dC}{dt} \right) = KAC \quad (17)$$

According to (İrdemez et al., 2006), the preceding equation can be expressed as equation (18).

$$V \ln\left(\frac{C_0}{C_t}\right) = KAt \quad (18)$$

$$\ln(C_t) = \left(\frac{-KA}{V}\right)t + \ln(C_0) \quad (19)$$

Here, V denotes the volume of the solution, C<sub>0</sub> the initial phosphorus concentration and C<sub>t</sub> the phosphorus concentration at any given time, K the removal rate constant, A the active electrode surface area and t the time. The variation of total phosphorus concentration with time is shown in Figure 22. It demonstrates that the kinetic data for the phosphorus removal was well fitted by the first order rate equation (K=0.185 m/min).

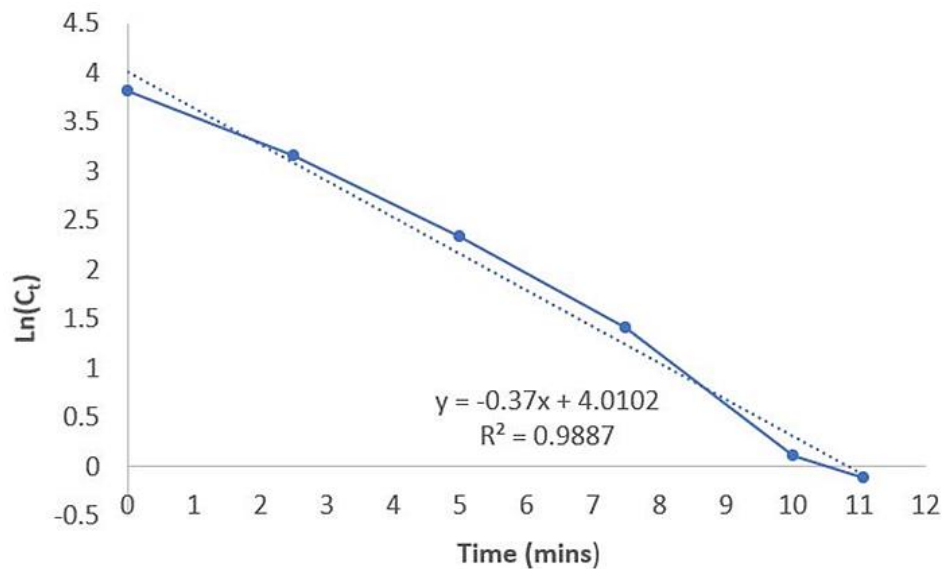


**Figure 22: Ln(C<sub>t</sub>) vs time**

#### 4.4.2 Magnesium Electrocoagulation System

The kinetics of total phosphorus removal at optimal operating conditions (pH = 8.4, retention time = 35 mins, current density = 300A/m<sup>2</sup>, inter-electrode distance = 0.5 cm) using electrochemical struvite precipitation can be expressed using the given second order rate law.

$$-V \left( \frac{dC}{dt} \right) = KAC^2 \quad (20)$$

The aforementioned equation upon integration can be expressed as equation (21).

$$V \left( \frac{1}{C_t} - \frac{1}{C_0} \right) = KAt \quad (21)$$

$$\frac{1}{C_t} = \frac{1}{C_0} + \frac{KA}{V} t \quad (22)$$

Here V is the volume of the solution, C<sub>0</sub> is the initial TP concentration, C<sub>t</sub> is the TP concentration at any given time, A is the anode surface area, K is the removal rate constant and t is the retention time. Figure 23 depicts a plot of the reciprocal of the TP concentration (mg/L) on the y-axis versus time (minutes) on the primary axis. It shows that the kinetic data for phosphorus removal was well fitted to the second-order rate equation (K=0.0117 mg/(m<sup>2</sup>·min)).

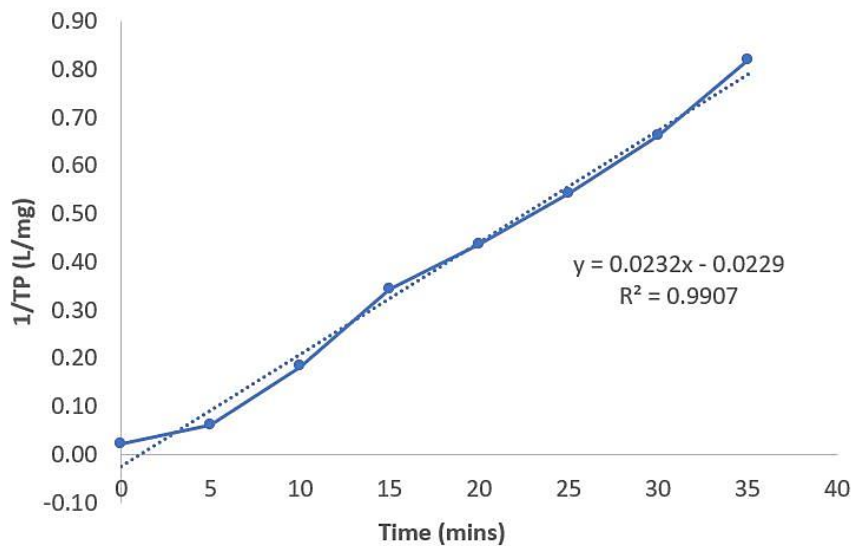


Figure 23: 1/TP vs time

## 4.5 Acid Leaching

Acid leaching tests were carried out for the iron electrocoagulation sludge obtained during optimum experimental conditions using sulphuric acid. Sulphuric acid is widely used in industry for phosphorus extraction from phosphate rock due to its high strength and proton donating ability (Atienza-Martínez et al., 2014). Leaching of phosphorus at an acid load of 100 kg/kg P and various liquid-to-solid (L/S) ratios is shown in Figure (19). It represents phosphorus yield for sludge combusted at 900 °C. This sludge ash has a phosphorus content of  $15.97 \pm 0.72$  % by mass. At an acid load of 100 kg/kg P and an L/S ratio of 100 mL/g, phosphorus recovery of more than 90% was observed. When the L/S ratio increased to 150 mL/g, the phosphorus concentration in the leachate decreased. The observed phosphorus recovery was greater than 75% for an L/S ratio of 200 mL/g. For an L/S ratio of 50 mL/g, a phosphorus recovery of 82% was observed. The concentration of sulphuric acid affects the acid leaching process. The molarity of sulphuric acid decreases as the liquid-to-solid ratio increases while the acid load remains constant. The dissolution of phosphorus in the leachate is influenced by the solution pH and L/S ratio. As an acid's molarity increases, its pH decreases. A decrease in pH causes an increase in phosphorus dissolution for a post-precipitated electrocoagulation sludge (Monea et al., 2020). An increase in the liquid-to-solid ratio for a constant sulphuric acid concentration causes an increase in phosphorus solubility for the post-precipitated electrocoagulation sludge over a 24-hour period (Damaraju et al., 2019). The phosphorus

dissolution is affected by changes in the L/S ratio and molarity of the acid simultaneously.

In this study, an L/S ratio of 100 mL/g was found to be optimal.

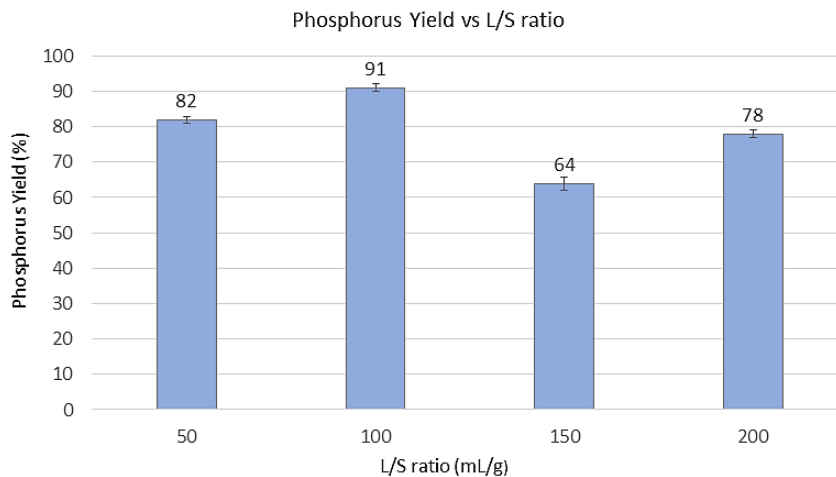


**Figure 24: Effect of L/S ratio on phosphorus yield**

## 5. Conclusions, Recommendations and Applications to Practice

### 5.1 Conclusions

The first research objective of the study was to compare the phosphorus recovery performance of iron and magnesium electrocoagulation systems. This objective was successfully achieved through the electrocoagulation study for total phosphorus recovery using iron and magnesium electrodes.

The second objective of this study was to evaluate the potential of the electrocoagulation process to remove phosphorus from anaerobic bioreactor's effluent under various operating conditions (initial pH, retention time, current density, and inter-electrode distance). It was observed that varying the operating conditions for electrocoagulation has a significant impact on phosphorus recovery. The ANOVA results depict the significance of the factors. The most significant model terms for both iron and magnesium electrocoagulation systems are shown in Table 17.

**Table 17: Significant factors for EC systems**

Model Term	Significant Factor	
	Iron EC System	Magnesium EC System
Linear	pH	RT
Square	pH <sup>2</sup>	pH <sup>2</sup>
2-Way Interaction	pH·CD	pH·RT

The third objective of the study was to conduct a statistical optimization of independent process variables and to model response and prediction using response surface methodology (RSM). To describe the behaviour of the operating parameters,

experimental data were fitted to a quadratic equation using multiple regression analysis. The predicted  $R^2$  value for iron and magnesium electrocoagulation systems was found to be 96.27% and 91.53% respectively. Statistical optimization of independent process variables predicted complete TP removal for iron and magnesium electrocoagulation system, whereas removal efficiencies of 98.05% and 97.30% were observed during experimental conditions.

The fourth objective of the study was to recover phosphorus from the precipitates formed during the iron electrocoagulation system using combustion followed by an acid leaching process. Acid leaching was affected by the molarity of the acid and the L/S ratio. The optimum combination of these parameters resulted in 91% TP recovery from the iron electrocoagulation sludge obtained under optimum operating conditions.

The final objective of the study was to evaluate the impact of electrocoagulation on COD removal for iron and magnesium electrodes, as well as the impact of a magnesium electrocoagulation system on ammonia removal. Results for both iron and magnesium electrocoagulation systems revealed that COD removal was very low compared to that of total phosphorus removal. This was because of the low initial COD concentration. For the magnesium electrocoagulation system, the maximum ammonia removal observed was around 31%.

## 5.2 Recommendations for Future Work

A list of recommendations is made based on the results obtained during this study.

- More research should be carried out to study the electrode passivation and the effect of electrode polarity reversal on the performance of an electrocoagulation reactor.
- Construction of a continuous flow reactor to study its performance for a higher sample volume using optimized data from the batch reactor and integration into existing treatment systems.
- Research on automation of the electrocoagulation process can provide great potential for its industrial application.

### 5.3 Applications to Practice

The results obtained from this study present potential for the anaerobic wastewater treatment facility. It provides an insight into the strategy for recovering phosphorus from nutrient-rich wastewater typically leaving anaerobic digesters/bioreactors treating municipal and industrial wastewaters via electrocoagulation process. Magnesium electrodes would be preferable over iron electrodes because the precipitate from this system does not require the complex phosphorus extraction process (combustion and acid leaching) that is required for iron electrodes. Ammonia concentration is a key parameter affecting the performance of the Mg-EC system. External ammonia addition will be required for anaerobic effluents with low ammonia concentration in order to achieve high phosphorus recovery efficiency. The most important factor influencing the mechanism and efficiency of electrocoagulation is the initial pH. The optimization data obtained from this study will be useful for the construction of continuous flow EC reactors for phosphorus recovery from anaerobic digestors and bioreactor effluent. The

response surface optimization includes interactions of the variables which would help in achieving the desired phosphorus recovery goals at a lower value of the variables thereby reducing energy consumption.

## REFERENCES

- American Public Health Association, Eaton, A. D., American Water Works Association, & Water Environment Federation. (2005). *Standard methods for the examination of water and wastewater* (21st ed.). APHA-AWWA-WEF.
- Asselin, M., Drogui, P., Benmoussa, H., & Blais, J.-F. (2008). Effectiveness of electrocoagulation process in removing organic compounds from slaughterhouse wastewater using monopolar and bipolar electrolytic cells. *Chemosphere*, 72(11), 1727–1733.  
<https://doi.org/10.1016/j.chemosphere.2008.04.067>
- Atlantic Canada Wastewater Guidelines Manual for Collection, Treatment, and Disposal, Environment Canada (2006). Retrieved July 20, 2022, from <https://novascotia.ca/nse/water/docs/AtlCanStdGuideSewage.pdf>
- Attour, A., Touati, M., Tlili, M., Ben Amor, M., Lopicque, F., & Leclerc, J.-P. (2014). Influence of operating parameters on phosphate removal from water by electrocoagulation using aluminum electrodes. *Separation and Purification Technology*, 123, 124–129. <https://doi.org/10.1016/j.seppur.2013.12.030>
- Bakshi, A., Verma, A. K., & Dash, A. K. (2020). Electrocoagulation for removal of phosphate from aqueous solution: Statistical modeling and techno-economic

study. *Journal of Cleaner Production*, 246, 118988.

<https://doi.org/10.1016/j.jclepro.2019.118988>

Bektaş, N., Akbulut, H., Inan, H., & Dimoglo, A. (2004). Removal of phosphate from aqueous solutions by electro-coagulation. *Journal of Hazardous Materials*, 106(2), 101–105. <https://doi.org/10.1016/j.jhazmat.2003.10.002>

Bernal-Martínez, L. A., Barrera-Díaz, C., Natividad, R., & Rodrigo, M. A. (2013). Effect of the continuous and pulse in situ iron addition onto the performance of an integrated electrochemical–ozone reactor for wastewater treatment. *Fuel*, 110, 133–140. <https://doi.org/10.1016/j.fuel.2012.11.067>

Bezerra, M. A., Santelli, R. E., Oliveira, E. P., Villar, L. S., & Escaleira, L. A. (2008). Response surface methodology (RSM) as a tool for optimization in analytical chemistry. *Talanta*, 76(5), 965–977.

<https://doi.org/10.1016/j.talanta.2008.05.019>

Booker, N. A., Priestley, A. J., & Fraser, I. H. (1999). Struvite Formation in Wastewater Treatment Plants: Opportunities for Nutrient Recovery. *Environmental Technology*, 20(7), 777–782. <https://doi.org/10.1080/09593332008616874>

Bowker, R. P. G., & Stensel, H. D. (1990). *Phosphorus removal from wastewater*. Noyes Data Corp.

Calvo, L. S., Leclerc, J.-P., Tanguy, G., Cames, M. C., Paternotte, G., Valentin, G., Rostan, A., & Lopicque, F. (2003). An electrocoagulation unit for the purification of soluble oil wastes of high COD. *Environmental Progress*, 22(1), 57–65.

<https://doi.org/10.1002/ep.670220117>

- Carmona-Carmona, P. F., Linares-Hernández, I., Teutli-Sequeira, E. A., López-Rebollar, B. M., Álvarez-Bastida, C., Mier-Quiroga, M. de L. A., Vázquez-Mejía, G., & Martínez-Miranda, V. (2021). Industrial wastewater treatment using magnesium electrocoagulation in batch and continuous mode. *Journal of Environmental Science and Health. Part A, Toxic/Hazardous Substances & Environmental Engineering*, 56(3), 269–288. <https://doi.org/10.1080/10934529.2020.1868823>
- Damaraju, M., Yoshihara, H., Bhattacharyya, D., Panda, T. K., & Kurilla, K. K. (2019). Phosphorus recovery from the sludge generated from a continuous bipolar mode electrocoagulation (CBME) system. *Water Science and Technology: A Journal of the International Association on Water Pollution Research*, 79(7), 1348–1356. <https://doi.org/10.2166/wst.2019.131>
- Devlin, T. R., Kowalski, M. S., Pagaduan, E., Zhang, X., Wei, V., & Oleszkiewicz, J. A. (2019). Electrocoagulation of wastewater using aluminum, iron, and magnesium electrodes. *Journal of Hazardous Materials*, 368, 862–868. <https://doi.org/10.1016/j.jhazmat.2018.10.017>
- Doyle, J. D., & Parsons, S. A. (2002). Struvite formation, control and recovery. *Water Research*, 36(16), 3925–3940. [https://doi.org/10.1016/S0043-1354\(02\)00126-4](https://doi.org/10.1016/S0043-1354(02)00126-4)
- Gaurina-Medjimurec, N. 1957-. (2015). *Handbook of research on advancements in environmental engineering* (Vol. 1–1 online resource.). Engineering Science Reference, an imprint of IGI Global; WorldCat.org.
- Gharibi, H., Mahvi, A. H., Chehrazi, M., Sheikhi, R., & Hosseini, S. S. (2010). Phosphorous removal from wastewater effluent using electro-coagulation by aluminum and

iron plates. *Analytical and Bioanalytical Electrochemistry*, 2(3), 165–177.

Scopus.

Ghosh, D., Medhi, C. R., & Purkait, M. K. (2008). Treatment of fluoride containing drinking water by electrocoagulation using monopolar and bipolar electrode connections. *Chemosphere*, 73(9), 1393–1400.

<https://doi.org/10.1016/j.chemosphere.2008.08.041>

Hakizimana, J. N., Gourich, B., Chafi, M., Stiriba, Y., Vial, C., Drogui, P., & Naja, J. (2017). Electrocoagulation process in water treatment: A review of electrocoagulation modeling approaches. *Desalination*, 404, 1–21.

<https://doi.org/10.1016/j.desal.2016.10.011>

Hermann, L., Kraus, F., & Hermann, R. (2018). Phosphorus Processing—Potentials for Higher Efficiency. *Sustainability*, 10(5), 1482.

<https://doi.org/10.3390/su10051482>

Holt, P. K., Barton, G. W., Wark, M., & Mitchell, C. A. (2002). A quantitative comparison between chemical dosing and electrocoagulation. *Colloids and Surfaces A: Physicochemical and Engineering Aspects*, 211(2), 233–248.

[https://doi.org/10.1016/S0927-7757\(02\)00285-6](https://doi.org/10.1016/S0927-7757(02)00285-6)

Huang, H., Zhang, D., Zhao, Z., Zhang, P., & Gao, F. (2017). Comparison investigation on phosphate recovery from sludge anaerobic supernatant using the electrocoagulation process and chemical precipitation. *Journal of Cleaner Production*, 141, 429–438. <https://doi.org/10.1016/j.jclepro.2016.09.127>

- İrdemez, Ş., Yildiz, Y. Ş., & Tosunoğlu, V. (2006). Optimization of phosphate removal from wastewater by electrocoagulation with aluminum plate electrodes. *Separation and Purification Technology*, 52(2), 394–401.  
<https://doi.org/10.1016/j.seppur.2006.05.020>
- Jiang, J.-Q., Graham, N., André, C., Kelsall, G. H., & Brandon, N. (2002). Laboratory study of electro-coagulation–flotation for water treatment. *Water Research*, 36(16), 4064–4078. [https://doi.org/10.1016/S0043-1354\(02\)00118-5](https://doi.org/10.1016/S0043-1354(02)00118-5)
- Johnston, A. E., Poulton, P. R., Fixen, P. E., & Curtin, D. (2014). Chapter Five - Phosphorus: Its Efficient Use in Agriculture. In D. L. Sparks (Ed.), *Advances in Agronomy* (Vol. 123, pp. 177–228). Academic Press.  
<https://doi.org/10.1016/B978-0-12-420225-2.00005-4>
- Kataki, S., West, H., Clarke, M., & Baruah, D. C. (2016). Phosphorus recovery as struvite: Recent concerns for use of seed, alternative Mg source, nitrogen conservation and fertilizer potential. *Resources, Conservation and Recycling*, 107, 142–156.  
<https://doi.org/10.1016/j.resconrec.2015.12.009>
- Kékedy-Nagy, L., Teymouri, A., Herring, A. M., & Greenlee, L. F. (2020). Electrochemical removal and recovery of phosphorus as struvite in an acidic environment using pure magnesium vs. The AZ31 magnesium alloy as the anode. *Chemical Engineering Journal*, 380, 122480. <https://doi.org/10.1016/j.cej.2019.122480>
- Khandegar, V., & Saroha, A. K. (2013). Electrocoagulation for the treatment of textile industry effluent – A review. *Journal of Environmental Management*, 128, 949–963. <https://doi.org/10.1016/j.jenvman.2013.06.043>

- Khemis, M., Tanguy, G., Leclerc, J. P., Valentin, G., & Lopicque, F. (2005). Electrocoagulation for the Treatment of Oil Suspensions: Relation Between the Rates of Electrode Reactions and the Efficiency of Waste Removal. *Process Safety and Environmental Protection*, 83(1), 50–57.  
<https://doi.org/10.1205/psep.03381>
- Kobyas, M., Demirbas, E., Can, O. T., & Bayramoglu, M. (2006). Treatment of levafix orange textile dye solution by electrocoagulation. *Journal of Hazardous Materials*, 132(2), 183–188. <https://doi.org/10.1016/j.jhazmat.2005.07.084>
- Kuehl, R. O. (2000). *Design of experiments : statistical principles of research design and analysis* (2nd ed.). Duxbury/Thomson Learning.
- Kyle, M. A., & McClintock, S. A. (1995). The availability of phosphorus in municipal wastewater sludge as a function of the phosphorus removal process and sludge treatment method. *Water Environment Research : A Research Publication of the Water Environment Federation (USA)*.
- Lacasa, E., Cañizares, P., Sáez, C., Fernández, F. J., & Rodrigo, M. A. (2011). Electrochemical phosphates removal using iron and aluminium electrodes. *Chemical Engineering Journal*, 172(1), 137–143.  
<https://doi.org/10.1016/j.cej.2011.05.080>
- Le Corre, K. S., Valsami-Jones, E., Hobbs, P., & Parsons, S. A. (2009). Phosphorus Recovery from Wastewater by Struvite Crystallization: A Review. *Critical Reviews in Environmental Science and Technology*, 39(6), 433–477.  
<https://doi.org/10.1080/10643380701640573>

- Linares-Hernández, I., Barrera-Díaz, C., Bilyeu, B., Juárez-GarcíaRojas, P., & Campos-Medina, E. (2010). A combined electrocoagulation–electrooxidation treatment for industrial wastewater. *Journal of Hazardous Materials*, *175*(1–3), 688–694. <https://doi.org/10.1016/j.jhazmat.2009.10.064>
- Mollah, M. Y. A., Schennach, R., Parga, J. R., & Cocke, D. L. (2001). Electrocoagulation (EC)—Science and applications. *Journal of Hazardous Materials*, *84*(1), 29–41. [https://doi.org/10.1016/S0304-3894\(01\)00176-5](https://doi.org/10.1016/S0304-3894(01)00176-5)
- Monea, M. C., Löhr, D. K., Meyer, C., Preyl, V., Xiao, J., Steinmetz, H., Schönberger, H., & Drenkova-Tuhtan, A. (2020). Comparing the leaching behavior of phosphorus, aluminum and iron from post-precipitated tertiary sludge and anaerobically digested sewage sludge aiming at phosphorus recovery. *Journal of Cleaner Production*, *247*, 119129. <https://doi.org/10.1016/j.jclepro.2019.119129>
- Montgomery, D. C. (1999). Experimental Design for Product and Process Design and Development. *Journal of the Royal Statistical Society: Series D (The Statistician)*, *48*(2), 159–177. <https://doi.org/10.1111/1467-9884.00179>
- Münch, E. V., & Barr, K. (2001). Controlled struvite crystallisation for removing phosphorus from anaerobic digester sidestreams. *Water Research*, *35*(1), 151–159. [https://doi.org/10.1016/S0043-1354\(00\)00236-0](https://doi.org/10.1016/S0043-1354(00)00236-0)
- Nasr, F. A., Sadik, M. A., & El-Shafai, S. (2019). Innovative Electrochemical Treatment of Textile Dye Wastewater. *Egyptian Journal of Chemistry*, *62*(11), 2019–2032. <https://doi.org/10.21608/ejchem.2019.10576.1683>

Ohlinger, K. N., P. E., N., Young, T. M., & Schroeder, E. D. (1999). Kinetics Effects on Preferential Struvite Accumulation in Wastewater. *Journal of Environmental Engineering*, 125(8), 730–737. [https://doi.org/10.1061/\(ASCE\)0733-9372\(1999\)125:8\(730\)](https://doi.org/10.1061/(ASCE)0733-9372(1999)125:8(730))

Ohlinger, K. N., Young, T. M., & Schroeder, E. D. (1998). Predicting struvite formation in digestion. *Water Research*, 32(12), 3607–3614. [https://doi.org/10.1016/S0043-1354\(98\)00123-7](https://doi.org/10.1016/S0043-1354(98)00123-7)

Ostara Nutrient Recovery Technologies Inc. (2017). Retrieved April 15, 2022, from [http://ostara.com/wp-content/uploads/2017/03/Ostara\\_NRS\\_BROCHURE\\_170328.pdf](http://ostara.com/wp-content/uploads/2017/03/Ostara_NRS_BROCHURE_170328.pdf)

Phalakornkule, C., Polgumhang, S., & Tongdaung, W. (2009). Performance of an Electrocoagulation Process in Treating Direct Dye: Batch and Continuous Upflow Processes. *International Journal of Chemical and Molecular Engineering*, 3(9), 499–504.

P-Rex. (2015). AirPrex® Struvite crystallization in sludge. Retrieved March 15, 2022, from <https://zenodo.org/record/242550/files/Technical%20Factsheets.pdf>

Rout, P. R., Bhunia, P., & Dash, R. R. (2014). Modeling isotherms, kinetics and understanding the mechanism of phosphate adsorption onto a solid waste: Ground burnt patties. *Journal of Environmental Chemical Engineering*, 3(2), 1331–1342. <https://doi.org/10.1016/j.jece.2014.04.017>

- Sahu, O., Mazumdar, B., & Chaudhari, P. K. (2014). Treatment of wastewater by electrocoagulation: A review. *Environmental Science and Pollution Research*, 21(4), 2397–2413. <https://doi.org/10.1007/s11356-013-2208-6>
- Sasson, M. B., Calmano, W., & Adin, A. (2009). Iron-oxidation processes in an electroflocculation (electrocoagulation) cell. *Journal of Hazardous Materials*, 171(1), 704–709. <https://doi.org/10.1016/j.jhazmat.2009.06.057>
- Schnug, E., & De Kok, L. J. (2016). *Phosphorus in Agriculture: 100 % Zero*. Springer Netherlands.
- Sengupta, S., Nawaz, T., & Beaudry, J. (2015). Nitrogen and Phosphorus Recovery from Wastewater. *Current Pollution Reports*, 1(3), 155–166. <https://doi.org/10.1007/s40726-015-0013-1>
- Shankar, R., Singh, L., Mondal, P., & Chand, S. (2014). Removal of COD, TOC, and color from pulp and paper industry wastewater through electrocoagulation. *Desalination and Water Treatment*, 52(40–42), 7711–7722. <https://doi.org/10.1080/19443994.2013.831782>
- Sridhar, R., Sivakumar, V., Prince Immanuel, V., & Prakash Maran, J. (2011). Treatment of pulp and paper industry bleaching effluent by electrocoagulant process. *Journal of Hazardous Materials*, 186(2), 1495–1502. <https://doi.org/10.1016/j.jhazmat.2010.12.028>
- Stratful, I., Brett, S., Scrimshaw, M. B., & Lester, J. N. (1999). Biological Phosphorus Removal, Its Role in Phosphorus Recycling. *Environmental Technology*, 20(7), 681–695. <https://doi.org/10.1080/09593332008616863>

- Stumm, W., & Morgan, J. J. (1996). *Aquatic chemistry: Chemical equilibria and rates in natural waters*. Wiley.
- Tran, N., Drogui, P., Blais, J.-F., & Mercier, G. (2012). Phosphorus removal from spiked municipal wastewater using either electrochemical coagulation or chemical coagulation as tertiary treatment. *Separation and Purification Technology*, *95*, 16–25. <https://doi.org/10.1016/j.seppur.2012.04.014>
- Ueno, Y., & Fujii, M. (2001). Three Years Experience of Operating and Selling Recovered Struvite from Full-Scale Plant. *Environmental Technology*, *22*(11), 1373–1381. <https://doi.org/10.1080/09593332208618196>
- Vaneckhaute, C., Lebuf, V., Michels, E., Belia, E., Vanrolleghem, P. A., Tack, F. M. G., & Meers, E. (2017). Nutrient Recovery from Digestate: Systematic Technology Review and Product Classification. *Waste and Biomass Valorization*, *8*(1), 21–40. <https://doi.org/10.1007/s12649-016-9642-x>
- Vasudevan, S., Lakshmi, J., & Sozhan, G. (2009). Optimization of the process parameters for the removal of phosphate from drinking water by electrocoagulation. *Desalination and Water Treatment*, *12*(1–3), 407–414. <https://doi.org/10.5004/dwt.2009.971>
- Yuan, Z., Pratt, S., & Batstone, D. J. (2012). Phosphorus recovery from wastewater through microbial processes. *Current Opinion in Biotechnology*, *23*(6), 878–883. <https://doi.org/10.1016/j.copbio.2012.08.001>

Zaveri, R. M., & Flora, J. R. V. (2002). Laboratory septic tank performance response to electrolytic stimulation. *Water Research*, 36(18), 4513–4524.

[https://doi.org/10.1016/S0043-1354\(02\)00152-5](https://doi.org/10.1016/S0043-1354(02)00152-5)

Zeng, J., Ji, M., Zhao, Y., Helmer Pedersen, T., & Wang, H. (2021). Optimization of electrocoagulation process parameters for enhancing phosphate removal in a biofilm-electrocoagulation system. *Water Science and Technology*, 83(10),

2560–2574. <https://doi.org/10.2166/wst.2021.132>

Zhang, T., Bowers, K. E., Harrison, J. H., & Chen, S. (2010). Releasing Phosphorus from Calcium for Struvite Fertilizer Production from Anaerobically Digested Dairy

Effluent. *Water Environment Research*, 82(1), 34–42.

<https://doi.org/10.2175/106143009X425924>

Zhang, X., Lin, H., & Hu, B. (2016). Phosphorus removal and recovery from dairy manure by electrocoagulation. *RSC Advances*, 6(63), 57960–57968.

<https://doi.org/10.1039/C6RA06568F>

## Appendix A: TP Data

**Table 18: TP data: Iron EC runs**

Run Order	Variables				Initial TP Concentration (mg/L)	Final TP Concentration (mg/L)
	pH	RT (mins)	CD (A/m <sup>2</sup> )	IED (cm)		
1	4.75	7.5	150	0.75	45.6 ± 2	42.19
2	8.25	7.5	150	0.75	45.6 ± 2	12.39
3	4.75	12.5	150	0.75	45.6 ± 2	29.15
4	8.25	12.5	150	0.75	45.6 ± 2	3.98
5	4.75	7.5	250	0.75	45.6 ± 2	29.83
6	8.25	7.5	250	0.75	45.6 ± 2	7.26
7	4.75	12.5	250	0.75	45.6 ± 2	14.85
8	8.25	12.5	250	0.75	45.6 ± 2	1.40
9	4.75	7.5	150	1.25	45.6 ± 2	33.25
10	8.25	7.5	150	1.25	45.6 ± 2	13.00
11	4.75	12.5	150	1.25	45.6 ± 2	29.15
12	8.25	12.5	150	1.25	45.6 ± 2	6.38
13	4.75	7.5	250	1.25	45.6 ± 2	17.47
14	8.25	7.5	250	1.25	45.6 ± 2	3.46
15	4.75	12.5	250	1.25	45.6 ± 2	9.83
16	8.25	12.5	250	1.25	45.6 ± 2	0.53
17	3	10	200	1	45.6 ± 2	43.14
18	10	10	200	1	45.6 ± 2	6.49
19	6.5	5	200	1	45.6 ± 2	26.42
20	6.5	15	200	1	45.6 ± 2	6.20
21	6.5	10	100	1	45.6 ± 2	23.15
22	6.5	10	300	1	45.6 ± 2	3.94
23	6.5	10	200	0.5	45.6 ± 2	10.71
24	6.5	10	200	1.5	45.6 ± 2	8.03
25	6.5	10	200	1	45.6 ± 2	10.31
26	6.5	10	200	1	45.6 ± 2	9.06
27	6.5	10	200	1	45.6 ± 2	8.34
28	6.5	10	200	1	45.6 ± 2	9.14
29	6.5	10	200	1	45.6 ± 2	6.53
30	6.5	10	200	1	45.6 ± 2	8.82
31	6.5	10	200	1	45.6 ± 2	7.99

\*Initial TP concentration includes the Mean ± SD of all the initial TP measurement

**Table 19: TP data: Magnesium EC runs**

Run Order	Variables				Initial TP	Final TP
	pH	RT (mins)	CD (A/m <sup>2</sup> )	IED (cm)	Concentration n (mg/L)	Concentration n (mg/L)
1	7.5	20	150	0.75	45.6 ± 2	6.98
2	9.5	20	150	0.75	45.6 ± 2	3.78
3	7.5	30	150	0.75	45.6 ± 2	3.43
4	9.5	30	150	0.75	45.6 ± 2	2.28
5	7.5	20	250	0.75	45.6 ± 2	4.51
6	9.5	20	250	0.75	45.6 ± 2	2.64
7	7.5	30	250	0.75	45.6 ± 2	2.30
8	9.5	30	250	0.75	45.6 ± 2	1.86
9	7.5	20	150	1.25	45.6 ± 2	5.40
10	9.5	20	150	1.25	45.6 ± 2	3.32
11	7.5	30	150	1.25	45.6 ± 2	3.19
12	9.5	30	150	1.25	45.6 ± 2	2.23
13	7.5	20	250	1.25	45.6 ± 2	3.27
14	9.5	20	250	1.25	45.6 ± 2	2.31
15	7.5	30	250	1.25	45.6 ± 2	1.93
16	9.5	30	250	1.25	45.6 ± 2	1.83
17	6.5	25	200	1.00	45.6 ± 2	7.07
18	10.5	25	200	1.00	45.6 ± 2	3.73
19	8.5	15	200	1.00	45.6 ± 2	5.07
20	8.5	35	200	1.00	45.6 ± 2	1.19
21	8.5	25	100	1.00	45.6 ± 2	4.00
22	8.5	25	300	1.00	45.6 ± 2	1.75
23	8.5	25	200	0.50	45.6 ± 2	2.92
24	8.5	25	200	1.50	45.6 ± 2	1.89
25	8.5	25	200	1.00	45.6 ± 2	2.51
26	8.5	25	200	1.00	45.6 ± 2	2.99
27	8.5	25	200	1.00	45.6 ± 2	2.60
28	8.5	25	200	1.00	45.6 ± 2	2.82
29	8.5	25	200	1.00	45.6 ± 2	3.26
30	8.5	25	200	1.00	45.6 ± 2	2.68
31	8.5	25	200	1.00	45.6 ± 2	2.75

\*Initial TP concentration includes the Mean ± SD of all the initial TP measurement

## Appendix B: EDS Analysis

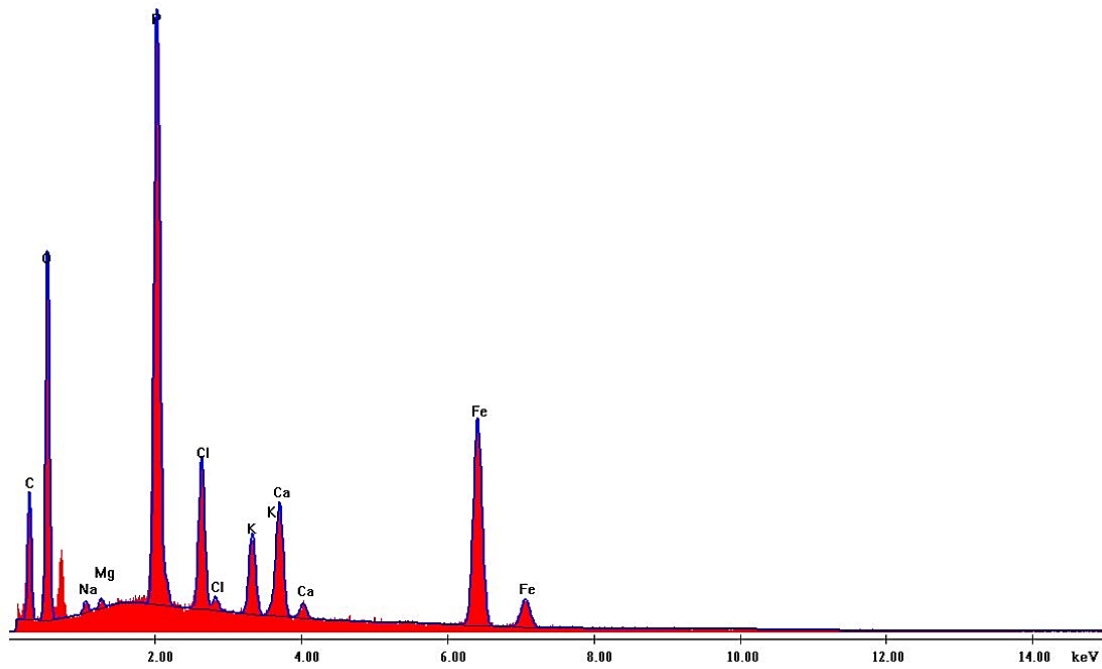


Figure 25: EDS analysis of the iron EC sludge

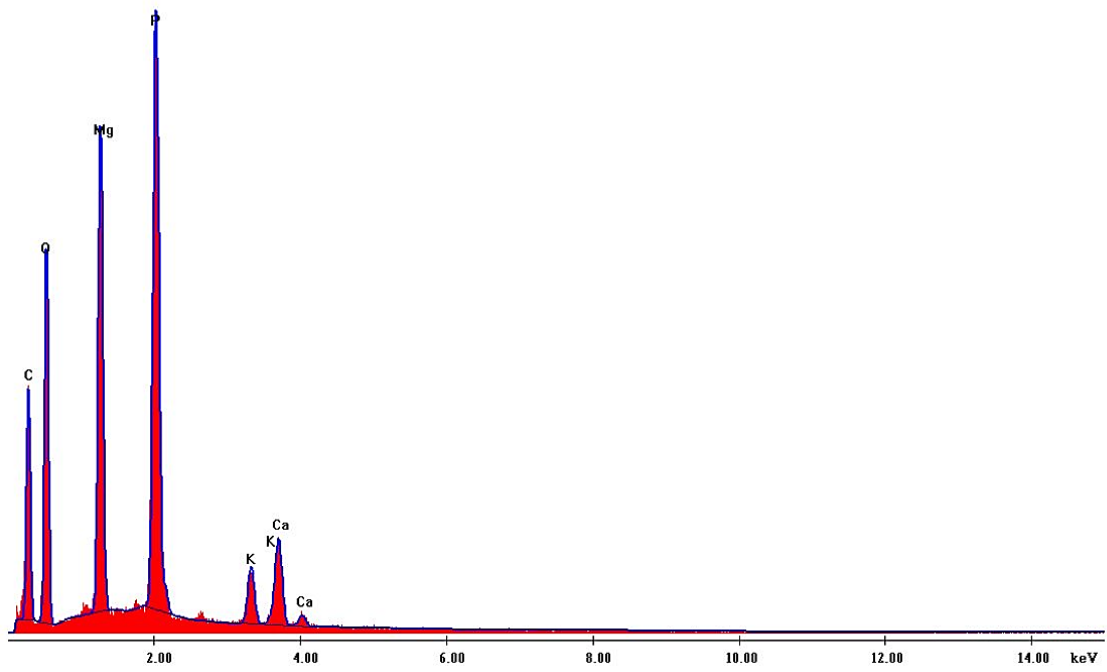


Figure 26: EDS analysis of the magnesium EC sludge

# Curriculum Vitae

**Candidate's full name:** Gyana Prakash Bhoi

## **Universities attended:**

University of New Brunswick, Fredericton, Canada      September 2019 – August 2022

MASTER OF SCIENCE IN CIVIL ENGINEERING

Biju Patnaik University of Technology, Rourkela, India      August 2015 – April 2019

BACHELOR OF TECHNOLOGY IN CIVIL ENGINEERING

## **Publications:**

Bhoi G. P., Singh, K. S., Connor, D. A. (2022). Phosphorus removal and recovery from anaerobic bioreactor effluent using a batch electrocoagulation process, *Water Quality Research Journal*.

Under Peer review.

## **Conference Presentations:**

Bhoi G. P., Singh, K. S. (2021). Phosphorus recovery from anaerobic bioreactor effluent using a batch monopolar electrocoagulation system. Conference proceedings from the 2021 Virtual Atlantic and Eastern Canadian Symposium on Water Quality Research.